

A UNIFIED APPROACH TO INTERPRETING AND BOOSTING ADVERSARIAL TRANSFERABILITY

Xin Wang^{a,*}, Jie Ren^{a,*}, Shuyun Lin^a, Xiangming Zhu^a, Yisen Wang^b, Quanshi Zhang^{a†}

^aShanghai Jiao Tong University, ^bPeking University

ABSTRACT

In this paper, we use the interaction inside adversarial perturbations to explain and boost the adversarial transferability. We discover and prove the negative correlation between the adversarial transferability and the interaction inside adversarial perturbations. The negative correlation is further verified through different DNNs with various inputs. Moreover, this negative correlation can be regarded as a unified perspective to understand current transferability-boosting methods. To this end, we prove that some classic methods of enhancing the transferability essentially decrease interactions inside adversarial perturbations. Based on this, we propose to directly penalize interactions during the attacking process, which significantly improves the adversarial transferability.

1 INTRODUCTION

Adversarial examples of deep neural networks (DNNs) have attracted increasing attention in recent years (Carlini & Wagner, 2017; Madry et al., 2018). Goodfellow et al. (2014); Liu et al. (2016) explored the transferability of adversarial perturbations, and used perturbations generated on a source DNN to attack other target DNNs. Although many methods have been proposed to enhance the transferability of adversarial perturbations (Dong et al., 2018; Wu et al., 2018; 2020), the essence of the improvement of the transferability is still unclear.

This paper considers the interaction inside adversarial perturbations as a new perspective to interpret adversarial transferability. Interactions inside adversarial perturbations are defined in game theory (Michel & Marc, 1999; Shapley, 1953). Given an input sample $x \in \mathbb{R}^n$, the adversarial attack aims to fool the DNN by adding an imperceptible perturbation $\delta \in \mathbb{R}^n$ on x . Each unit in the perturbation map is termed a *perturbation unit*. Let ϕ_i denote the importance of the i -th perturbation unit δ_i to attacking. ϕ_i is implemented as the Shapley value, which will be explained later. The interaction between perturbation units δ_i, δ_j is defined as the change of the i -th unit's importance ϕ_i when the j -th unit is perturbed *w.r.t* the case when the j -th unit is not perturbed. If the perturbation δ_j on the j -th unit increases the importance ϕ_i of the i -th unit, then there is a positive interaction between δ_i and δ_j . If the perturbation δ_j decreases the importance ϕ_i , it indicates a negative interaction.

In this paper, we discover and partially prove the strong negative correlation between the transferability and the interaction between adversarial perturbation units, *i.e.* adversarial perturbations with lower transferability tend to exhibit larger interactions between perturbation units. We verify such a correlation based on both the theoretical proof and comparative studies. Furthermore, based on the correlation, we propose to penalize interactions during attacking to improve the transferability.

The background for us to investigate the correlation between adversarial transferability and the interaction is as follows. First, we prove that multi-step attacking usually generates perturbations with larger interactions than single-step attacking. Second, according to (Xie et al., 2019), multi-step attacking tends to generate more over-fitted adversarial perturbations with lower transferability than single-step attacking. We consider that the more dedicated interaction reflects more over-fitting towards the source DNN, which hurts adversarial transferability. In this way, we propose the hypothesis that *the transferability and the interaction are negatively correlated*.

*Equal contribution

†Correspondence.

- **Comparative studies** are conducted to verify this negative correlation through different DNNs.
- **Unified explanation.** Such a negative correlation provides a unified view to understand current transferability-boosting methods. We theoretically prove that some classic transferability-boosting methods (Dong et al., 2018; Wu et al., 2018; 2020) essentially decrease interactions between perturbation units, which also verifies the hypothesis of the negative correlation.
- **Boosting adversarial transferability.** Based on above findings, we propose a loss to decrease interactions between perturbation units during attacking, namely the interaction loss, in order to enhance the adversarial transferability. The effectiveness of the interaction loss further proves the negative correlation between the adversarial transferability and the interaction inside adversarial perturbations. Furthermore, we also try to only use the interaction loss to generate perturbations without the loss for the classification task. We find that such perturbations still exhibit moderate adversarial transferability for attacking. Such perturbations may decrease interactions encoded by the DNN, thereby damaging the inference patterns of the input.

Our contributions are summarized as follows. (1) We reveal the negative correlation between the transferability and the interaction inside adversarial perturbations. (2) We provide a unified view to understand current transferability-boosting methods. (3) We propose a new loss to penalize interactions inside adversarial perturbations and enhance the adversarial transferability.

2 RELATED WORK

Adversarial transferability. Attacking methods can be roughly divided into two categories, *i.e.* white-box attacks (Szegedy et al., 2013; Goodfellow et al., 2014; Papernot et al., 2016; Carlini & Wagner, 2017; Kurakin et al., 2017; Su et al., 2017; Madry et al., 2018) and black-box attacks (Liu et al., 2016; Papernot et al., 2017; Chen et al., 2017; Bhagoji et al., 2018; Ilyas et al., 2018; Jiang et al., 2019). A specific type of the black-box attack is based on the adversarial transferability (Dong et al., 2018; Wu et al., 2018; Xie et al., 2019; Wu et al., 2020), which transfers adversarial perturbations on a surrogate/source DNN to a target DNN.

Thus, some previous studies focused on the transferability of adversarial attacking. Liu et al. (2016) demonstrated that non-targeted attacks were easy to transfer, while the targeted attacks were difficult to transfer. Wu et al. (2018) and Demontis et al. (2019) explored factors influencing the transferability, such as network architectures, model capacity, and gradient alignment. Several methods have been proposed to enhance the transferability of adversarial perturbations. The momentum iterative attack (MI Attack) (Dong et al., 2018) incorporated the momentum of gradients to boost the transferability. The variance-reduced attack (VR Attack) (Wu et al., 2018) used the smoothed gradients to craft perturbations with high transferability. The diversity input attack (DI Attack) (Xie et al., 2019) applied the adversarial attacking to randomly transformed input images, which included random resizing and padding with a certain probability. The skip gradient method (SGM Attack) (Wu et al., 2020) used the gradients of the skip connection to improve the transferability. Dong et al. (2019) proposed the translation-invariant attack (TI Attack) to evade robustly trained DNNs. Li et al. (2020) used the dropout erosion and the skip connection erosion to improve the transferability.

In comparison, we explain the transferability based on game theory, and discover the negative correlation between the transferability and interactions as a unified explanation for some above methods.

Interaction. The interaction between input variables has been widely investigated. Daria Sorokina (2008) defined the interaction of K input variables of additive models. Scott Lundberg (2017) quantified interactions between each pair of input variables for tree-ensemble models. Some studies mainly focused on interactions to analyze DNNs. Tsang et al. (2018) measured statistical interactions based on DNN weights. Murdoch et al. (2018) proposed to extract interactions in LSTMs by disambiguating information of different gates, and Singh et al. (2019) extended this method to CNNs. Jin et al. (2020) quantified the contextual independence of words to hierarchically explain the LSTMs. In comparison, in this study, we use a different type of interactions based on game theory, in order to explain and improve the transferability of adversarial perturbations.

3 THE RELATIONSHIP BETWEEN TRANSFERABILITY AND INTERACTIONS

Preliminaries: the Shapley value. The Shapley value was first proposed in game theory (Shapley, 1953). Considering multiple players in a game, each player aims to win a high reward. The Shapley value is considered as a unique and unbiased approach to fairly allocating the total reward gained by all players to each player (Weber, 1988). The Shapley value satisfies four desirable properties, *i.e.* the *linearity*, *dummy*, *symmetry*, and *efficiency* (please see the Appendix A for details). Let $\Omega = \{1, 2, \dots, n\}$ denote the set of all players, and let $v(\cdot)$ denote the reward function. $v(S)$ represents the reward obtained by a set of players $S \subseteq \Omega$. The Shapley value $\phi(i|\Omega)$ unbiasedly measures the contribution of the i -th player to the total reward gained by all players in Ω , as follows.

$$\sum_i \phi(i|\Omega) = v(\Omega) - v(\emptyset), \quad \phi(i|\Omega) = \sum_{S \subseteq \Omega \setminus \{i\}} \frac{|S|! (n - |S| - 1)!}{n!} (v(S \cup \{i\}) - v(S)). \quad (1)$$

Adversarial attack. Given an input sample $x \in [0, 1]^n$ with the true label $y \in \{1, 2, \dots, C\}$, we use $h(x) \in \mathbb{R}^C$ to denote the output of the DNN before the softmax layer. To simplify the story, in this study, we mainly focus on the untargeted adversarial attack. The goal of the untargeted adversarial attack is to add a human-imperceptible perturbation $\delta \in \mathbb{R}^n$ on the sample x , and make the DNN classify the perturbed sample $x' = x + \delta$ into an incorrect category, *i.e.* $\arg \max_{y'} h_{y'}(x') \neq y$. The objective of adversarial attacking is usually formulated as follows.

$$\max_{\delta} \ell(h(x + \delta), y) \quad \text{s.t.} \quad \|\delta\|_p \leq \epsilon, \quad x + \delta \in [0, 1]^n, \quad (2)$$

where $\ell(h(x + \delta), y)$ is referred to as the classification loss, and ϵ is a constant of the norm constraint. Please see Appendix C for technical details of solving Equation (2).

3.1 THEORETICAL UNDERSTANDING OF THE ADVERSARIAL ATTACK IN GAME THEORY.

In adversarial attacking, given the perturbation $\delta \in \mathbb{R}^n$, we use $\Omega = \{1, 2, \dots, n\}$ to denote all units/dimensions in the perturbation. We use the Shapley value in Equation (1) to measure the contribution of each perturbation unit $i \in \Omega$ to the attack. To this end, it requires us to define the utility of a subset of perturbation units $S \subseteq \Omega$ for attacking, which can be formulated as $v(S) = \max_{y' \neq y} h_{y'}(x + \delta^{(S)}) - h_y(x + \delta^{(S)})$, according to Equation (2). $h_y(\cdot)$ is the value of the y -th element of $h(\cdot) \in \mathbb{R}^C$. $\delta^{(S)} \in \mathbb{R}^n$ is the perturbation which only contains perturbation units in S , *i.e.* $\forall i \in S, \delta_i^{(S)} = \delta_i; \forall i \notin S, \delta_i^{(S)} = 0$. In this way, $v(\Omega) = \max_{y' \neq y} h_{y'}(x + \delta) - h_y(x + \delta)$ denotes the utility of all perturbation units, and $v(\emptyset) = \max_{y' \neq y} h_{y'}(x) - h_y(x)$ denotes the baseline score without perturbations. Thus, the overall contribution of perturbation units can be measured as $v(\Omega) - v(\emptyset)$. We apply the Shapley value in Equation (1) to assign the overall contribution to each perturbation unit as $\sum_i \phi(i|\Omega) = v(\Omega) - v(\emptyset)$, where $\phi(i|\Omega)$ denotes the contribution of the i -th perturbation unit.

Interactions. Perturbation units do not contribute to the adversarial utility independently. For example, perturbation units may form a certain pattern, *e.g.* an edge in the image. Thus, perturbations units in the edge must appear together. The absence of a few units in the pattern may invalidate this pattern. Let us consider two perturbation units i, j . According to (Michel & Marc, 1999), the interaction between units i, j is defined as the additional contribution as follows.

$$I_{ij}(\delta) = \phi(S_{ij}|\Omega') - [\phi(i|\Omega \setminus \{j\}) + \phi(j|\Omega \setminus \{i\})], \quad (3)$$

where $\phi(i|\Omega \setminus \{j\})$ and $\phi(j|\Omega \setminus \{i\})$ represent the individual contributions of units i and j , respectively, when the perturbation units i, j work individually. Note that $\phi(i|\Omega \setminus \{j\})$ is computed in the scenario of considering the unit j always absent. $\sum_i \phi(i|\Omega \setminus \{j\}) = v(\Omega \setminus \{j\}) - v(\emptyset)$, due to the absence of perturbation unit j . $\phi(S_{ij}|\Omega')$ denotes the joint contribution of i, j , when perturbation units i, j are regarded as a singleton unit $S_{ij} = \{i, j\}$. In this case, units i, j are supposed to be always perturbed or not perturbed simultaneously, and we can consider that there are only $n - 1$ players in the game. Thus, the set of all perturbation units is considered as $\Omega' = \Omega \setminus \{i, j\} \cup S_{ij}$. The joint contribution of S_{ij} is denoted by $\phi(S_{ij}|\Omega')$, s.t. $\sum_{i' \in \Omega' \setminus \{S_{ij}\}} \phi(i'|\Omega') + \phi(S_{ij}|\Omega') = v(\Omega') - v(\emptyset)$.

The interaction defined in Equation (3) is equivalent to the change of the i -th unit's importance ϕ_i when the unit j exists *w.r.t* the case when the unit j is absent. Please see Appendix D for the proof.

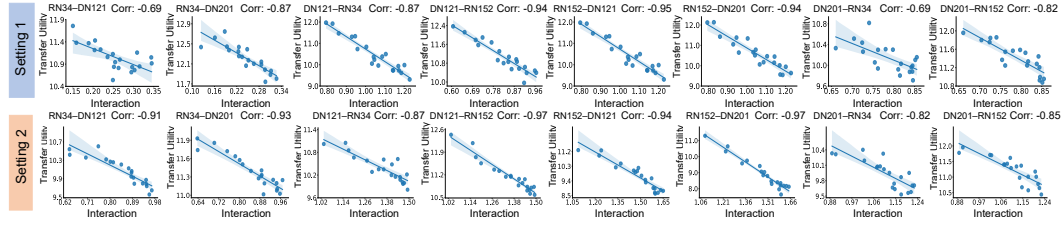


Figure 1: The negative correlation between the transfer utility and the interaction. The correlation is computed as the Pearson correlation. The blue shade in each subfigure represents the 95% confidence interval of the linear regression.

If $I_{ij}(\delta) > 0$, it means δ_i and δ_j cooperate with each other, *i.e.* the interaction is positive; if $I_{ij}(\delta) < 0$, it means δ_i and δ_j conflict with each other, *i.e.* the interaction is negative. The absolute value of $|I_{ij}(\delta)|$ indicates the interaction strength. The interaction is symmetric that $I_{ij}(\delta) = I_{ji}(\delta)$.

With the definition of interactions, in adversarial attacking, we have the following propositions:

Proposition 1. (Proof in Appendix E) Given an input sample $x \in \mathbb{R}^n$ and a DNN $h(\cdot)$ trained for classification, the adversarial perturbation generated by the multi-step attack via gradient descent is given as $\delta_{\text{multi}}^m = \alpha \sum_{t=0}^{m-1} \nabla_x \ell(h(x + \delta_{\text{multi}}^t), y)$, where δ_{multi}^t denotes the perturbation after the t -th step of updating, and m is referred to as the total number of steps. The adversarial perturbation generated by the single-step attack is given as $\delta_{\text{single}} = \alpha m \nabla_x \ell(h(x), y)$. Then, the expectation of interactions between perturbation units in δ_{multi}^m , $\mathbb{E}_{a,b}[I_{ab}(\delta_{\text{multi}}^m)]$, is larger than $\mathbb{E}_{a,b}[I_{ab}(\delta_{\text{single}})]$, *i.e.* $\mathbb{E}_{a,b}[I_{ab}(\delta_{\text{multi}}^m)] \geq \mathbb{E}_{a,b}[I_{ab}(\delta_{\text{single}})]$.

Note that when we compare interactions inside different perturbations, magnitudes of these perturbations should be similar. It is because the comparison of interactions between adversarial perturbations of different magnitudes is not fair. Therefore, we use the step size αm in the single-step attack to roughly (not accurately) balance the magnitude of perturbations. The fairness is further discussed in Appendix E.1.

Proposition 1 shows that, in general, adversarial perturbations generated by the multi-step attack tend to exhibit larger interactions than those generated by the single-step attack. In addition, Appendix E.4 shows that the multi-step attack usually generates perturbations with larger interactions than noisy perturbations of the same magnitude. Besides, Xie et al. (2019) demonstrated that the multi-step attack tends to over-fit the source DNN, which led to low transferability. Intuitively, large interactions mean a strong cooperative relationship between perturbation units, which indicates the significant over-fitting towards adversarial perturbations oriented to the source DNN. In this way, we propose the hypothesis that *the adversarial transferability and the interactions inside adversarial perturbations are negatively correlated*.

3.2 EMPIRICAL VERIFICATION OF THE NEGATIVE CORRELATION

To verify the negative correlation between the transferability and interactions, we conduct experiments to examine whether adversarial perturbations with low transferability tend to exhibit larger interactions than those perturbations with high transferability. Given a source DNN and an input sample x , we generate the adversarial example $x' = x + \delta$. Then, given a target DNN $h^{(t)}$, we measure the transfer utility of δ as $\text{Transfer Utility} = [\max_{y' \neq y} h_{y'}^{(t)}(x + \delta) - h_y^{(t)}(x + \delta)] - [\max_{y' \neq y} h_{y'}^{(t)}(x) - h_y^{(t)}(x)]$ as mentioned in Section 3.1. The interaction is given as $\text{Interaction} = \mathbb{E}_{i,j}[I_{ij}(\delta)]$, which is computed on the source DNN. Note that the computational cost of $I_{ij}(\delta)$ is NP-hard. However, we prove that we can simplify the computation of the average interaction over all pairs of units as follows, which significantly reduces the computational cost. Please see Appendix F for the proof.

$$\mathbb{E}_{i,j}[I_{ij}(\delta)] = \frac{1}{n-1} \mathbb{E}_i[v(\Omega) - v(\Omega \setminus \{i\}) - v(\{i\}) + v(\emptyset)]. \quad (4)$$

Using the validation set of the ImageNet dataset (Russakovsky et al., 2015), we generate adversarial perturbations on four types of DNNs, including ResNet-34/152(RN-34/152) (He et al., 2016) and

DenseNet-121/201(DN-121/201) (Huang et al., 2017). We transfer adversarial perturbations generated on each ResNet to DenseNets. Similarly, we also transfer adversarial perturbations generated on each DenseNet to ResNets. Figure 1 shows the negative correlation between the transfer utility and the interaction. Each subfigure corresponds to a specific pair of source DNN and target DNN. In each subfigure, each point represents the average transfer utility and the average interaction of adversarial perturbations through all testing images. Different points represent the average interaction and the average transfer utility computed using different hyper-parameters. Given an input image x , adversarial perturbations are generated by solving the relaxed form of Equation (2) via the gradient descent, *i.e.* $\min_{\delta} -\ell(h(x + \delta), y) + c \cdot \|\delta\|_p^p$ s.t. $x + \delta \in [0, 1]^n$, where $c \in \mathbb{R}$ is a scalar. In this way, we gradually change the value of c and set different values of p^1 as different hyper-parameters to generate different adversarial perturbations, thereby drawing different points in each subfigure. Fair comparisons require adversarial perturbations generated with different hyper-parameters c to be comparable with each other. Thus, we select a constant τ and take $\|\delta\|_2 = \tau$ as the stopping criteria of all adversarial attacks. The selection of τ is discussed in Appendix H.

4 UNIFIED UNDERSTANDING OF TRANSFERABILITY-BOOSTING ATTACKS

In this section, we prove that some classical methods of improving the adversarial transferability essentially decrease interactions between perturbation units, although these methods are not originally designed to decrease the interaction.

• **VR Attack** (Wu et al., 2018) smooths the classification loss with the Gaussian noise during attacking. In the VR Attack, the gradient of the input sample is computed as follows. $g^t = \mathbb{E}_{\xi \sim \mathcal{N}(0, \sigma^2 I)} [\nabla_x \ell(h(x + \delta^t + \xi), y)]$. The following proposition proves that the VR Attack is prone to decrease interactions inside perturbation units.

Proposition 2. (Proof in Appendix I) *Given an input image $x \in \mathbb{R}^n$ and a DNN $h(\cdot)$ trained for classification, the adversarial perturbation generated by the multi-step attack is given as $\delta_{multi}^m = \alpha \sum_{t=0}^{m-1} \nabla_x \ell(h(x + \delta_{multi}^t), y)$. The adversarial perturbation generated by the VR Attack is computed as $\delta_{vr}^m = \alpha \sum_{t=0}^{m-1} \nabla_x \hat{\ell}(h(x + \delta_{vr}^t), y)$, where $\hat{\ell}(h(x + \delta_{vr}^t), y) = \mathbb{E}_{\xi \sim \mathcal{N}(0, \sigma^2 I)} [\ell(h(x + \delta_{vr}^t + \xi), y)]$. Perturbation units of δ_{vr}^m tend to exhibit smaller interactions than δ_{multi}^m , *i.e.* $\mathbb{E}_x \mathbb{E}_{a,b} [I_{ab}(\delta_{vr}^m)] \leq \mathbb{E}_x \mathbb{E}_{a,b} [I_{ab}(\delta_{multi}^m)]$.*

Besides the theoretical proof, we also conduct experiments to compare interactions of perturbation units generated by the baseline multi-step attack (implemented as (Madry et al., 2018)) with those of perturbation units generated by the VR Attack. Table 4 shows that the VR Attack exhibits lower interactions between perturbation units than the baseline multi-step attack.

• **MI Attack** (Dong et al., 2018) incorporates the momentum of gradients when updating the adversarial perturbation. In the MI Attack, the gradient used in step t is computed as follows. $g^t = \mu \cdot g^{t-1} + \nabla_x \ell(h(x + \delta^{t-1}), y) / \|\nabla_x \ell(h(x + \delta^{t-1}), y)\|_1$.

Note that the original MI Attack and the multi-step attack cannot be directly compared, since that magnitudes of the generated perturbations cannot be fairly controlled. The value of interactions is sensitive to the magnitude of perturbations. Comparing perturbations with different magnitudes is not fair. Thus, we slightly revise the MI Attack as $\forall t > 0, g_{mi}^t = \mu g_{mi}^{t-1} + (1 - \mu) \nabla_x \ell(h(x + \delta_{mi}^{t-1}), y); g_{mi}^0 = 0$, where $\mu = (t - 1)/t$. We investigate the interaction of adversarial perturbations generated by the original multi-step attack and the MI Attack. We prove the following proposition, which shows that the MI Attack decreases the interaction between perturbation units in most cases.

Proposition 3. (Proof in Appendix J) *Given an input sample $x \in \mathbb{R}^n$ and a DNN $h(\cdot)$ trained for classification, the adversarial perturbation generated by the multi-step attack is given as $\delta_{multi}^m = \alpha \sum_{t=0}^{m-1} \nabla_x \ell(h(x + \delta_{multi}^t), y)$. The adversarial perturbation generated by the multi-step attack incorporating the momentum is computed as $\delta_{mi}^m = \alpha \sum_{t=0}^{m-1} g_{mi}^t$. Perturbation units of δ_{mi}^m exhibit smaller interactions than δ_{multi}^m , *i.e.* $\mathbb{E}_{a,b} [I_{ab}(\delta_{mi}^m)] \leq \mathbb{E}_{a,b} [I_{ab}(\delta_{multi}^m)]$.*

¹We set $p = 2$ as the setting 1, and $p = 5$ as the setting 2. To this end, the performance of adversarial perturbations is not the key issue in the experiment. Instead, we just randomly set the p value to examine the trustworthiness of the negative correlation under various attacking conditions (even in extreme attacking conditions).

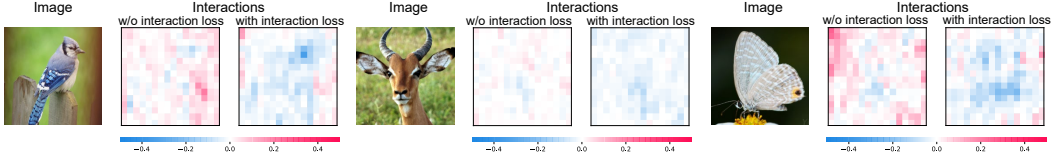


Figure 2: Visualization of interactions between neighboring perturbation units generated with and without the interaction loss. The color in the visualization is computed as $color[i] \propto E_{j \in N_i} [I_{ij}(\delta)]$, where N_i denotes the set of adjacent perturbation units of the perturbation unit i . Here, we ignore interactions between non-adjacent units to simplify the visualization. It is because adjacent units usually encode much more significant interactions than other units. The interaction loss forces the perturbation to encode more negative interactions.

• **SGM Attack** (Wu et al., 2020) exploits the gradient information of the skip connection in ResNets to improve the transferability of adversarial perturbations. The SGM Attack revises the gradient in the backpropagation, which can be considered as to add a specific dropout operation in the backpropagation. We notice that Zhang et al. (2020) prove that the dropout operation can decrease the significance of interactions, so as to decrease the significance of the over-fitting of DNNs. Thus, this also proves that the SGM Attack decreases interactions between perturbation units.

Besides the theoretical proof, we also conduct experiments to compare interactions of perturbation units generated by the baseline multi-step attack (implemented as Madry et al. (2018)) with those of perturbation units generated by the SGM Attack. Table 4 shows that the SGM Attack exhibits lower interactions than the baseline multi-step attack.

5 THE INTERACTION LOSS FOR TRANSFERABILITY ENHANCEMENT

Interaction loss. Based on findings in previous sections, we propose a loss to directly penalize interactions during attacking, in order to improve the transferability of adversarial perturbations. Based on Equation (2), we jointly optimize the classification loss and the interaction loss to generate adversarial perturbations. This method is termed the interaction-reduced attack (IR Attack).

$$\max_{\delta} [\ell(h(x + \delta), y) - \lambda \ell_{\text{interaction}}], \quad \ell_{\text{interaction}} = \mathbb{E}_{i,j} [I_{ij}(\delta)] \quad \text{s.t. } \|\delta\|_p \leq \epsilon, \quad x + \delta \in [0, 1]^n, \quad (5)$$

where $\ell_{\text{interaction}}$ is the interaction loss, and λ is a constant weight for the interaction loss. Although the computation of the interaction loss can be simplified according to Equation (4), the computational cost of the interaction loss is intolerable, when the dimension of images is high. Therefore, as a trade-off between the accuracy and the computational cost, we divide the input image into 16×16 grids. We measure and penalize interactions at the grid level, instead of the pixel level. Figure 2 visualizes interactions between adjacent perturbation units at the grid level generated with and without the interaction loss.

Experiments. For implementation, we generated adversarial perturbations on six different source DNNs, including Alexnet (Krizhevsky et al., 2012), VGG-16 (Simonyan & Zisserman, 2015), ResNet-34/152 (RN-34/152) (He et al., 2016) and DenseNet-121/201 (DN-121/201) (Huang et al., 2017). For each source DNN, we tested the transferability of the generated perturbations on seven target DNNs, including VGG-16, ResNet-152 (RN-152), DenseNet-201 (DN-201), SENet-154 (SE-154) (Hu et al., 2018), InceptionV3 (IncV3) (Szegedy et al., 2016), InceptionV4 (IncV4) (Szegedy et al., 2017), and Inception-ResNetV2 (IncResV2) (Szegedy et al., 2017). Besides above seven unsecured target DNNs, we also used three secured target models for testing, which were learned via ensemble adversarial training: IncV3_{ens3} (ensemble of three IncV3 networks), IncV3_{ens4} (ensemble of four IncV3 networks), and IncResV2_{ens3} (ensemble of three IncResV2 networks), which were released by Tramèr et al. (2017).

Besides above adversarial transferring from a single-source model, we also conducted the proposed IR Attack in the scenario of the ensemble-based attacking (Liu et al., 2016), in order to generate adversarial perturbations on the ensemble of RN-34, RN-152, and DN-121.

Baselines. The first baseline method (Madry et al., 2018) directly solved the Equation (2), which had been simply termed the *Baseline* (this baseline method for attacking was also called the PGD Attack,

Table 1: The success rates of L_∞ and L_2 black-box attacks crafted by the baseline attack (Madry et al., 2018) and IR Attack methods on seven source models, including AlexNet, VGG16, RN-34/152, DN-121/201, the ensemble model (RN-34+RN-152+DN-121), against seven target models. Transferability of adversarial perturbations can be enhanced by penalizing interactions.

Source	Method	VGG16	RN-152	DN-201	SE-154	IncV3	IncV4	IncResV2		VGG16	RN-152	DN-201	SE-154	IncV3	IncV4	IncResV2
AlexNet	Baseline	63.4	28.0	34.7	28.1	26.6	24.4	17.9	L_∞ attack	83.6	59.7	58.1	53.4	53.5	46.1	44.3
	IR Attack	77.8	42.3	48.5	42.0	44.9	37.4	30.1		90.4	70.4	75.7	67.9	72.9	61.0	57.4
VGG16	Baseline	—	45.2	51.8	55.7	40.3	49.5	31.7	L_2 attack	—	75.7	81.3	82.3	74.7	80.1	31.7
	IR Attack	—	64.4	69.5	69.9	53.7	69.6	48.8		—	85.5	87.9	89.4	84.7	86.7	80.1
RN-34	Baseline	66.6	59.6	65.4	36.5	29.4	24.2	23.9	L_∞ attack	87.4	85.8	88.1	65.7	61.5	59.4	53.5
	IR Attack	85.4	85.1	86.0	65.4	56.4	54.2	49.1		95.0	94.2	96.1	85.4	83.7	79.7	78.2
RN-152	Baseline	55.5	—	63.6	40.4	26.0	27.7	22.3	L_2 attack	—	—	—	—	—	—	—
	IR Attack	71.6	—	80.6	64.0	53.6	50.3	48.0		—	—	—	—	—	—	—
DN-121	Baseline	67.3	66.3	88.6	44.8	35.5	38.3	29.1	L_∞ attack	88.2	87.1	96.4	73.8	66.9	64.9	61.1
	IR Attack	83.5	85.2	95.3	72.2	62.4	63.0	56.2		93.0	92.9	97.4	87.2	84.1	83.3	81.5
DN-201	Baseline	64.4	72.7	—	51.3	44.4	37.6	37.6	L_2 attack	—	—	—	—	—	—	—
	IR Attack	75.7	85.4	—	73.6	59.8	63.0	56.6		—	—	—	—	—	—	—
Ensemble model	Baseline	87.6	99.9	96.8	78.3	67.6	60.5	59.1	L_∞ attack	—	—	—	—	—	—	—
	IR Attack	92.3	94.1	94.0	86.2	80.6	78.0	78.4		—	—	—	—	—	—	—

Table 2: Transferability against the secured models: the success rates of L_∞ black-box attacks crafted on RN-34 and DN-121 source models against three secured models.

Source	Method	IncV3 _{ens3}	IncV3 _{ens4}	IncRes _{ens3}	Source	Method	IncV3 _{ens3}	IncV3 _{ens4}	IncRes _{ens3}
RN-34	Baseline	9.8	10.5	5.4	DN-121	Baseline	13.8	13.1	7.9
	IR	29.8	23.6	14.7		IR	26.0	24.1	15.9
	TI ³	22.1	21.5	16.1		TI ³	28.1	27.5	21.2
	TI ³ + IR	34.1	33.1	23.7		TI ³ + IR	40.9	51.0	30.6

which was widely used for adversarial attacks). Besides this baseline attack, the other four baselines were the MI Attack (Dong et al., 2018), the VR Attack (Wu et al., 2018), the SGM Attack (Wu et al., 2020), and the TI Attack (Dong et al., 2019). Our method was implemented according to Equation (5), namely the IR Attack. Because the SGM Attack was one of the top-ranked methods of boosting the adversarial transferability, we further added the interaction loss $\ell_{\text{interaction}}$ to the SGM Attack as another implementation of our method (namely the SGM+IR Attack). Moreover, as Section 4 states, the MI Attack, VR Attack, and SGM Attack also decrease interactions during attacking. Thus, we combined the IR Attack with all these interaction-reducing techniques together as a new implementation of our method, namely the HybridIR Attack. All attacks were conducted with 100 steps² on the validation set in the ImageNet dataset. We set $\epsilon = 16/255$ for the L_∞ attack and $\epsilon = 16\sqrt{n}/255$ for the L_2 attack, where n was the dimension of the image. The step size was set to $2/255$ for all attacks. Considering the efficiency of signal processing in DNNs with different depths, we set $\lambda = 1$ for the IR Attack, when the source DNN was ResNet, and set $\lambda = 2$, for other source DNNs. To enable fair comparisons, the transferability of each baseline was computed based on the best adversarial perturbation during the 100 steps via the leave-one-out (LOO) validation. Please see the Appendix M for the motivation and the evidence of the LOO evaluation of transferability.

Table 1 reports the success rates of the baseline attack (PGD (Madry et al., 2018)) and the IR Attack. Compared with the baseline attack, the transferability was significantly improved by the interaction loss on various source models against different target models. Let us focus on the L_∞ attack. For most source models and target models, the transferability enhancement brought by the interaction loss was more than 10%. In particular, when the source DNN and the target DNN were DN-201 and IncV4, respectively, the baseline attack achieved the transferability of 37.6%. With the interaction loss, the transferability was improved to 63.0% ($> 25\%$ gain). Besides, as Table 2 shows, our interaction loss also improved the transferability against the secured target DNNs. Such improvement further verified the negative correlation between transferability and interactions. Table 3 shows the improvement of the transferability obtained by the interaction loss on other attacking methods. The interaction loss could further boost the transferability of state-of-the-art transfer attacks. Without the interaction loss, the highest transferability made by the SGM Attack against the IncResV2 was

²Previous studies usually set the number of steps to 10 or 20. Here, we set the number of steps to 100 together with the leave-one-out validation for fair comparisons of different attacks.

³The TI Attack was designed oriented to the secured DNNs which were robustly trained via adversarial training. Thus, we applied the TI Attack to the secured models in Table 2.

Table 3: The success rates of L_∞ black-box attacks crafted by different methods on four source models (RN-34/152, DN-121/201) against seven target models.

	Method	VGG16	RN152	DN201	SE154	IncV3	IncV4	IncResV2		Method	VGG16	RN152	DN201	SE154	IncV3	IncV4	IncResV2
RN-34	MI	78.3	68.5	73.7	48.9	46.5	37.1	35.3	DN-121	MI	80.6	72.8	91.6	61.0	54.1	48.9	42.2
	VR	89.0	87.5	90.0	60.8	56.8	58.3	48.9		VR	91.5	89.3	98.6	74.1	74.9	79.0	71.1
	SGM	92.4	89.7	89.1	69.2	65.3	59.6	53.6		SGM	88.6	87.0	98.5	77.4	64.6	62.8	61.7
	SGM + IR	95.4	92.0	93.7	72.4	68.6	65.4	62.5		SGM + IR	91.6	90.1	94.3	86.7	77.4	79.5	77.5
	HybridIR	96.5	95.3	95.3	80.6	76.7	73.9	69.8		HybridIR	96.7	96.8	99.1	91.4	88.3	88.7	86.9
RN-152	MI	69.7	—	73.4	52.7	46.1	40.0	33.9	DN-201	MI	76.4	75.6	—	65.4	53.7	48.8	45.6
	VR	83.1	—	90.8	70.7	68.1	62.1	60.4		VR	88.5	89.0	—	77.4	77.6	76.3	71.8
	SGM	87.7	—	90.1	74.3	64.0	60.5	57.1		SGM	87.1	93.5	—	83.0	72.0	71.9	68.2
	SGM + IR	92.6	—	92.8	80.3	69.2	67.4	64.0		SGM + IR	89.1	91.1	—	86.0	82.0	80.6	81.2
	HybridIR	95.8	—	97.0	84.0	79.1	78.1	75.7		HybridIR	94.3	96.5	—	91.6	89.5	88.6	86.5

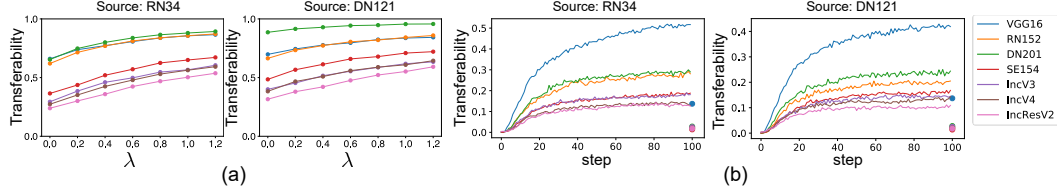


Figure 3: (a) The success rates of black-box attacks with the IR Attack using different values of λ . The success rates increased, when the value of λ increased. (b) The transferability of adversarial perturbations generated by only using the interaction loss (without the classification loss). Such adversarial perturbations still exhibited moderate adversarial transferability. Points localized at the last epoch represent the transferability of noise perturbations as the baseline.

68.2% (when the source is DN-201). When the interaction loss was added, the transferability was improved to 81.2% (13% gain). Moreover, the HybridIR Attack, which combined all methods of reducing interactions together, improved success rates from the range of 48.9%~98.5% to the range of 69.8%~99.1%.

Effects of the interaction loss. We tested the transferability of perturbations generated by the IR Attack with different weights of the interaction loss λ . In particular, the baseline attack can be considered as the IR Attack when $\lambda = 0$. We conducted attacks on two source DNNs (RN-34, DN-121), and transferred adversarial perturbations to seven target DNNs (VGG16, RN-152, DN-201, SE-154, IncV3, IncV4, IncResV2). The attacks were conducted with 100 steps² on validation images in ImageNet. Figure 3 (a) shows the black-box success rates with different values of λ . The transferability of the IR Attack increased along with the increase of the weight λ .

Attack only with the interaction loss. To further understand the effects of the interaction loss, we generated perturbations by exclusively using the interaction loss (without the classification loss). We used the RN-34 and DN-121 as source DNNs and tested the transferability on seven target DNNs. The attacks were conducted with 100 steps² on ImageNet validation images. Figure 3 (b) shows the curve of the transferability in different epochs. We compared such adversarial perturbations with noise perturbations generated as $\epsilon \cdot \text{sign}(\text{noise})$, where $\text{noise} \sim \mathcal{N}(0, \sigma^2 I)$, and $\epsilon = 16/255$, which was the same as the value used in the L_∞ attack. We found that perturbations generated by only using the interaction loss still exhibited moderate adversarial transferability. This phenomenon may be explained as that such perturbations decrease most interactions in the DNN, thereby damaging the inference patterns in the input image.

6 CONCLUSION

In this paper, we have analyzed the transferability of adversarial perturbations from the perspective of interactions based on game theory. We have proved that the multi-step attack tends to generate adversarial perturbations with large interactions. We have discovered and partially proved the negative correlation between the transferability and interactions inside adversarial perturbations. *I.e.* adversarial perturbations with higher transferability usually exhibit more negative interactions. We have proved that some classical methods of enhancing the transferability essentially decrease inter-

actions between perturbation units, which provides a unified view to understand the enhancement of transferability. Moreover, we propose a new loss to directly penalize interactions between perturbation units during attacking, which significantly improves the transferability of previous methods. Furthermore, we have found that adversarial perturbations generated only using the interaction loss without the classification loss still exhibited moderate transferability, which provides a new perspective to understand the transferability of adversarial perturbations.

REFERENCES

- Arjun Nitin Bhagoji, Warren He, Bo Li, and Dawn Song. Practical black-box attacks on deep neural networks using efficient query mechanisms. In *European Conference on Computer Vision*, pp. 158–174. Springer, 2018.
- Nicholas Carlini and David Wagner. Towards evaluating the robustness of neural networks. In *2017 IEEE Symposium on Security and Privacy (SP)*, pp. 39–57. IEEE, 2017.
- Jianbo Chen, Le Song, Martin J. Wainwright, and Michael I. Jordan. L-shapley and c-shapley: Efficient model interpretation for structured data. In *arXiv:1808.02610*, 2018a.
- Pin-Yu Chen, Huan Zhang, Yash Sharma, Jinfeng Yi, and Cho-Jui Hsieh. Zoo: Zeroth order optimization based black-box attacks to deep neural networks without training substitute models. In *arXiv:1708.03999*, 2017.
- Pin-Yu Chen, Yash Sharma, Huan Zhang, Jinfeng Yi, and Cho-Jui Hsieh. Ead: Elastic-net attacks to deep neural networks via adversarial examples. In *AAAI*, 2018b.
- Mirek Riedewald Daria Sorokina, Rich Caruana. Detecting statistical interactions with additive groves of trees. In *ICML*, 2008.
- Ambra Demontis, Marco Melis, Maura Pintor, Matthew Jagielski, Battista Biggio, Alina Oprea, Cristina Nita-Rotaru, and Fabio Roli. Why do adversarial attacks transfer? explaining transferability of evasion and poisoning attacks. In *28th USENIX Security Symposium USENIX Security 19*, pp. 321–338, 2019.
- Yinpeng Dong, Fangzhou Liao, Tianyu Pang, Hang Su, Xiaolin Hu, Jianguo Li, , and Jun Zhu. Boosting adversarial attacks with momentum. In *CVPR*, 2018.
- Yinpeng Dong, Tianyu Pang, Hang Su, and Jun Zhu. Evading defenses to transferable adversarial examples by translation-invariant attacks. In *Proceedings of the IEEE Conference on Computer Vision and Pattern Recognition*, pp. 4312–4321, 2019.
- Ian J Goodfellow, Jonathon Shlens, and Christian Szegedy. Explaining and harnessing adversarial examples. *arXiv preprint arXiv:1412.6572*, 2014.
- Kaiming He, Xiangyu Zhang, Shaoqing Ren, and Jian Sun. Deep residual learning for image recognition. In *CVPR*, 2016.
- Jie Hu, Li Shen, and Gang Sun. Squeeze-and-excitation networks. In *Proceedings of the IEEE conference on computer vision and pattern recognition*, pp. 7132–7141, 2018.
- Gao Huang, Zhuang Liu, Laurens Van Der Maaten, and Kilian Q Weinberger. Densely connected convolutional networks. In *Proceedings of the IEEE conference on computer vision and pattern recognition*, pp. 4700–4708, 2017.
- Qian Huang, Isay Katsman, Horace He, Zeqi Gu, Serge Belongie, and Ser-Nam Lim. Enhancing adversarial example transferability with an intermediate level attack. In *Proceedings of the IEEE International Conference on Computer Vision*, pp. 4733–4742, 2019.
- Andrew Ilyas, Logan Engstrom, Anish Athalye, and Jessy Lin. Black-box adversarial attacks with limited queries and information. In *ICML*, 2018.
- Nathan Inkawhich, Wei Wen, Hai Helen Li, and Yiran Chen. Feature space perturbations yield more transferable adversarial examples. In *Proceedings of the IEEE Conference on Computer Vision and Pattern Recognition*, pp. 7066–7074, 2019.
- Nathan Inkawhich, Kevin Liang, Lawrence Carin, and Yiran Chen. Transferable perturbations of deep feature distributions. In *International Conference on Learning Representations*, 2020.
- Linxi Jiang, Xingjun Ma, Shaoxiang Chen, James Bailey, and Yu-Gang Jiang. Black-box adversarial attacks on video recognition models. In *ACM MM*, 2019.

- Xisen Jin, Zhongyu Wei, Junyi Du, Xiangyang Xue, and Xiang Ren. Towards hierarchical importance attribution: Explaining compositional semantics for neural sequence models. *In ICLR*, 2020.
- Alex Krizhevsky, Geoffrey Hinton, et al. Learning multiple layers of features from tiny images. 2009.
- Alex Krizhevsky, Ilya Sutskever, and Geoffrey E Hinton. Imagenet classification with deep convolutional neural networks. pp. 1097–1105, 2012.
- Alexey Kurakin, Ian J. Goodfellow, and Samy Bengio. Adversarial examples in the physical world. *In arXiv:1607.02533*, 2017.
- Yingwei Li, Song Bai, Yuyin Zhou, Cihang Xie, Zhishuai Zhang, and Alan Yuille. Learning transferable adversarial examples via ghost networks. *In Proceedings of the AAAI Conference on Artificial Intelligence*, volume 34, 2020.
- Yanpei Liu, Xinyun Chen, Chang Liu, and Dawn Song. Delving into transferable adversarial examples and black-box attacks. *ICLR*, 2016.
- Aleksander Madry, Aleksandar Makelov, Ludwig Schmidt, Dimitris Tsipras, and Adrian Vladu. Towards deep learning models resistant to adversarial attacks. *In ICLR*, 2018.
- Grabisch Michel and Roubens Marc. An axiomatic approach to the concept of interaction among players in cooperative games. *In International Journal of Game Theory*, 1999.
- W. James Murdoch, Peter J. Liu, and Bin Yu. Beyond word importance: Contextual decomposition to extract interactions from lstms. *In ICLR*, 2018.
- Nicolas Papernot, Patrick McDaniel, Somesh Jha, Matt Fredrikson, Z. Berkay Celik, and Ananthram Swami. The limitations of deep learning in adversarial settings. *In IEEE European Symposium on Security & Privacy*, 2016.
- Nicolas Papernot, Patrick McDaniel, Ian Goodfellow, Somesh Jha, Z. Berkay Celik, and Ananthram Swami. Practical black-box attacks against machine learning. *In arXiv:1602.02697*, 2017.
- Olga Russakovsky, Jia Deng, Hao Su, Jonathan Krause, Sanjeev Satheesh, Sean Ma, Zhiheng Huang, Andrej Karpathy, Aditya Khosla, Michael Bernstein, Alexander C. Berg, and Li Fei-Fei. Imagenet large scale visual recognition challenge. *In International Journal of Computer Vision*, 115(3):211–252, 2015.
- Su-In Lee Scott Lundberg. Consistent feature attribution for tree ensembles. *In ICML WHI Workshop*, 2017.
- Lloyd S Shapley. A value for n-person games. *In Contributions to the Theory of Games*, 2(28): 307–317, 1953.
- Karen Simonyan and Andrew Zisserman. Very deep convolutional networks for large-scale image recognition. *In ICLR*, 2015.
- Chandan Singh, W. James Murdoch, and Bin Yu. Hierarchical interpretations for neural network predictions. *In ICLR*, 2019.
- Jiawei Su, Danilo Vasconcellos Vargas, and Sakurai Kouichi. One pixel attack for fooling deep neural networks. *In arXiv:1710.08864*, 2017.
- Christian Szegedy, Wojciech Zaremba, Ilya Sutskever, Joan Bruna, Dumitru Erhan, Ian Goodfellow, and Rob Fergus. Intriguing properties of neural networks. *arXiv preprint arXiv:1312.6199*, 2013.
- Christian Szegedy, Vincent Vanhoucke, Sergey Ioffe, Jon Shlens, and Zbigniew Wojna. Rethinking the inception architecture for computer vision. *In Proceedings of the IEEE conference on computer vision and pattern recognition*, pp. 2818–2826, 2016.

- Christian Szegedy, Sergey Ioffe, Vincent Vanhoucke, and Alexander A Alemi. Inception-v4, inception-resnet and the impact of residual connections on learning. In *Thirty-first AAAI conference on artificial intelligence*, 2017.
- Florian Tramèr, Alexey Kurakin, Nicolas Papernot, Ian Goodfellow, Dan Boneh, and Patrick McDaniel. Ensemble adversarial training: Attacks and defenses. *arXiv preprint arXiv:1705.07204*, 2017.
- Michael Tsang, Dehua Cheng, and Yan Liu. Detecting statistical interactions from neural network weights. In *ICLR*, 2018.
- Robert J Weber. Probabilistic values for games. *The Shapley Value. Essays in Honor of Lloyd S. Shapley*, pp. 101–119, 1988.
- Dongxian Wu, Yisen Wang, Shu-Tao Xia, James Bailey, and Xingjun Ma. Skip connections matter: On the transferability of adversarial examples generated with resnets. In *International Conference on Learning Representations*, 2020.
- Lei Wu, Zhanxing Zhu, and Cheng Tai. Understanding and enhancing the transferability of adversarial examples. *arXiv preprint arXiv:1802.09707*, 2018.
- Cihang Xie, Zhishuai Zhang, Yuyin Zhou, Song Bai, Jianyu Wang, Zhou Ren, and Alan L Yuille. Improving transferability of adversarial examples with input diversity. In *Proceedings of the IEEE Conference on Computer Vision and Pattern Recognition*, pp. 2730–2739, 2019.
- Hao Zhang, Sen Li, Yinchao Ma, Mingjie Li, Yichen Xie, and Quanshi Zhang. Interpreting and boosting dropout from a game-theoretic view. *arXiv preprint arXiv:2009.11729*, 2020.

A FOUR PROPERTIES OF SHAPLEY VALUES

Let $\Omega = \{1, 2, \dots, n\}$ denote the set of all players, and the reward function is v . Without ambiguity, we use $\phi(i|\Omega)$ to denote the Shapley value of the player i in the game with all players Ω and reward function v , which is given as follows.

$$\phi(i|\Omega) = \sum_{S \subseteq \Omega \setminus \{i\}} \frac{|S|!(n-|S|-1)!}{n!} (v(S \cup \{i\}) - v(S)). \quad (6)$$

The Shapley value satisfies the following four properties (Weber, 1988):

- *Linearity property*: If there are two games and the corresponding reward functions are v and w , i.e. $v(S)$ and $w(S)$ measure the reward obtained by players in S in these two games. Let $\phi_v(i|\Omega)$ and $\phi_w(i|\Omega)$ denote the Shapley value of the player i in the game v and game w , respectively. If these two games are combined into a new game, and the reward function becomes $\text{reward}(S) = v(S) + w(S)$, then the Shapley value comes to be $\phi_{v+w}(i|\Omega) = \phi_v(i|\Omega) + \phi_w(i|\Omega)$ for each player i in Ω .
- *Dummy property*: A player $i \in \Omega$ is referred to as a dummy player if $\forall S \subseteq \Omega \setminus \{i\}, v(S \cup \{i\}) = v(S) + v(\{i\})$. In this way, $\phi(i|\Omega) = v(\{i\}) - v(\emptyset)$, which means that player i plays the game independently.
- *Symmetry property*: If $\forall S \subseteq \Omega \setminus \{i, j\}, v(S \cup \{i\}) = v(S \cup \{j\})$, then Shapley values of player i and j are equal, i.e. $\phi(i|\Omega) = \phi(j|\Omega)$.
- *Efficiency property*: The sum of each individual's Shapley value is equal to the reward won by the coalition N , i.e. $\sum_i \phi(i|\Omega) = v(\Omega) - v(\emptyset)$. This property guarantees the overall reward can be allocated to each player in the game.

B COMPARISONS BETWEEN INTERACTIONS INSIDE PERTURBATIONS OF DIFFERENT ATTACKS

Table 4: The average interaction inside adversarial perturbations generated by different attacks.

Method	RN-34	RN-152	DN-121	DN-201
Baseline (PGD Attack)	0.422	0.926	0.909	0.784
SGM Attack	-0.012	0.037	0.395	0.308
VR Attack	0.097	0.270	0.242	0.137

We have theoretically proved that some classical attacking methods of boosting the adversarial transferability essentially decrease interactions inside perturbations. Besides the theoretical proof in Appendix J and Appendix I, we also conduct experiments to compare interactions of perturbation units when we generate adversarial perturbations with and without these attacking methods. Such experiments further verify that these methods of boosting the transferability essentially decrease interactions. We conduct attacks with the validation set in the ImageNet dataset on four DNNs, and measure the average interaction inside perturbation units. As Table 4 shows, the SGM Attack and the VR Attack decrease interactions inside perturbations.

C ADVERSARIAL ATTACK

In general, the objective of adversarial attacking can be formulated as the following optimization problem.

$$\underset{\delta}{\text{maximize}} \quad \ell(h(x + \delta), y) \quad \text{s.t.} \quad \|\delta\|_p \leq \epsilon, \quad x + \delta \in [0, 1]^n, \quad (7)$$

where $\ell(h(x + \delta), y)$ is the classification loss. There are many ways to solve the above optimization problem under different norm constraints $\|\cdot\|_p$ (Goodfellow et al., 2014; Carlini & Wagner, 2017; Kurakin et al., 2017; Madry et al., 2018; Chen et al., 2018b).

Optimization-based approach. One approach to approximately solving Equation (7) is to solve the following relaxed form:

$$\underset{\delta}{\text{minimize}} \quad \{-\ell(h(x + \delta), y) + c \cdot \|\delta\|_p\} \quad \text{s.t.} \quad x + \delta \in [0, 1]^n, \quad (8)$$

where $c > 0$ is a scalar constant to balance the classification loss and the norm constraint. Szegedy et al. (2013); Carlini & Wagner (2017) have demonstrated the effectiveness of this method.

Projected gradient descent (PGD) (Madry et al., 2018). The PGD Attack is usually considered as one of the simplest and the most widely used baseline for adversarial attacking. In this paper, this method is called the *Baseline*. The PGD Attack directly optimizes the classification loss in Equation (7). Considering the norm constraint, after each step of updating, the PGD Attack projects the adversarial perturbation δ back to the ϵ -ball, if the perturbation goes beyond the ball.

PGD updates adversarial perturbations in each step with the following equation:

$$\delta^{t+1} = \begin{cases} \Pi_{\epsilon}^{(\infty)}(\delta^t + \alpha \cdot \text{sign}(\nabla \ell(h(x + \delta^t), y))), & p = +\infty \\ \Pi_{\epsilon}^{(2)}\left(\delta^t + \alpha \cdot \frac{\nabla \ell(h(x + \delta^t), y)}{\|\nabla \ell(h(x + \delta^t), y)\|_2}\right), & p = 2, \end{cases} \quad (9)$$

where δ^t denotes the perturbation of the t -th step. $\Pi_{\epsilon}^{(\infty)}$ and $\Pi_{\epsilon}^{(2)}$ are projection operations, which project the perturbation δ back to the ϵ -ball, if the perturbation goes beyond the ball. α is the step size. Given $\delta \in \mathbb{R}^n$, we have:

$$\Pi_{\epsilon}^{(\infty)}(\delta_i) = \begin{cases} \epsilon \cdot \text{sign}(\delta_i), & \text{if } |\delta_i| > \epsilon \\ \delta_i, & \text{if } |\delta_i| \leq \epsilon \end{cases}, \quad \Pi_{\epsilon}^{(2)}(\delta) = \begin{cases} \epsilon \frac{\delta}{\|\delta\|_2}, & \text{if } \|\delta\|_2 > \epsilon \\ \delta, & \text{if } \|\delta\|_2 \leq \epsilon \end{cases}. \quad (10)$$

Interaction-reduced attack (IR Attack). Note that our interaction-reduced attack (IR Attack) uses the similar way as PGD Attack to iteratively update perturbations. The objective function of IR Attack is given as follows.

$$\underset{\delta}{\text{maximize}} \quad [\ell(h(x + \delta), y) - \lambda \cdot \mathbb{E}_{i,j} [I_{ij}(\delta)]] \quad \text{s.t.} \quad \|\delta\|_p \leq \epsilon, \quad x + \delta \in [0, 1]^n,$$

We optimize the objective of IR Attack as follows.

$$\delta^{t+1} = \begin{cases} \Pi_{\epsilon}^{(\infty)}(\delta^t + \alpha \cdot \text{sign}[\nabla \ell(h(x + \delta^t), y) - \lambda \cdot \nabla \mathbb{E}_{i,j}(\delta^t)]), & p = +\infty \\ \Pi_{\epsilon}^{(2)}\left(\delta^t + \alpha \cdot \frac{\nabla \ell(h(x + \delta^t), y) - \lambda \cdot \nabla \mathbb{E}_{i,j}(\delta^t)}{\|\nabla \ell(h(x + \delta^t), y) - \lambda \cdot \nabla \mathbb{E}_{i,j}(\delta^t)\|_2}\right), & p = 2 \end{cases} \quad (11)$$

D EQUIVALENT FORMS OF THE INTERACTION

In Section 3.1, the interaction between units i, j is defined as the additional contribution as follows.

$$I_{ij}(\delta) = \phi(S_{ij}|\Omega') - [\phi(i|\Omega \setminus \{j\}) + \phi(j|\Omega \setminus \{i\})], \quad (12)$$

where $\phi(i|\Omega \setminus \{j\})$ and $\phi(j|\Omega \setminus \{i\})$ represent the individual contributions of units i and j , respectively, when the perturbation units i, j work individually. $\phi(S_{ij}|\Omega')$ denotes the joint contribution of i, j , when perturbation units i, j are regarded as a singleton unit $S_{ij} = \{i, j\}$. Note that $\sum_i \phi(i|\Omega \setminus \{j\}) = v(\Omega \setminus \{j\}) - v(\emptyset)$, due to the absence of perturbation unit j .

In Section 1, the interaction between perturbation units δ_i, δ_j is defined as the change of the importance ϕ_i of the i -th unit when the j -th unit δ_j is perturbed *w.r.t* the case when the j -th unit δ_j is not perturbed. If the perturbation δ_j on the j -th unit increases the importance ϕ_i of the i -th unit, then there is a positive interaction between δ_i and δ_j . If the perturbation δ_j decreases the importance ϕ_i , it indicates a negative interaction. Mathematically, this definition can be written as follows.

$$I'_{ij}(\delta) = \phi_{i,w/j} - \phi_{i,w/o j}, \quad (13)$$

where $\phi_{i,w/j}$ represents the importance of δ_i , when δ_j is always present; $\phi_{i,w/o j}$ represents the importance of δ_i , when δ_j is always absent.

In this section, we aim to prove that the interaction in Equation (12) is equal to the interaction in Equation (13), *i.e.* $I_{ij}(\delta) = I'_{ij}(\delta)$.

Proof. In Equation (12), the interaction is give as $\phi(S_{ij}|\Omega') - [\phi(i|\Omega \setminus \{j\}) + \phi(j|\Omega \setminus \{i\})]$, where $\phi(S_{ij}|\Omega')$, $\phi(i|\Omega \setminus \{j\})$, and $\phi(j|\Omega \setminus \{i\})$ are implemented as Shapley values.

$$\phi(S_{ij}|\Omega') = \sum_{S \subseteq \Omega \setminus \{i,j\}} \frac{|S|!(n - |S| - 2)!}{(n - 1)!} (v(S \cup \{i, j\}) - v(S)),$$

where $S_{ij} = \{i, j\}$ represents the coalition of perturbation units i, j . In this game, because perturbation units i, j are regarded as a singleton player, we can consider there are only $n - 1$ players in the game, and consequently the set of players changes to $\Omega' = \Omega \setminus \{i, j\} \cup S_{ij}$.

The individual contribution of perturbation unit i , when perturbation unit j is absent, is given as follows.

$$\phi(i|\Omega \setminus \{j\}) = \sum_{S \subseteq \Omega \setminus \{i, j\}} \frac{|S|! (n - |S| - 2)!}{(n - 1)!} (v(S \cup \{i\}) - v(S)).$$

In this game, because the perturbation unit j is always absent, we can consider there are only $n - 1$ players in the game. Consequently the set of players changes to $\Omega \setminus \{j\}$.

The individual contribution of perturbation unit j , when perturbation unit i is absent, is given as follows.

$$\phi(j|\Omega \setminus \{i\}) = \sum_{S \subseteq \Omega \setminus \{i, j\}} \frac{|S|! (n - |S| - 2)!}{(n - 1)!} (v(S \cup \{j\}) - v(S)).$$

In this game, because the perturbation unit i is always absent, we can consider there are only $n - 1$ players in the game. Consequently the set of players changes to $\Omega \setminus \{i\}$.

In this way,

$$\begin{aligned} I_{ij}(\delta) &= \phi(S_{ij}|\Omega') - (\phi(i|\Omega \setminus \{j\}) + \phi(j|\Omega \setminus \{i\})) \\ &= \sum_{S \subseteq \Omega \setminus \{i, j\}} \frac{|S|! (n - |S| - 2)!}{(n - 1)!} \{v(S \cup \{i, j\}) - v(S) - [v(S \cup \{i\}) - v(S) + v(S \cup \{j\}) - v(S)]\} \\ &= \sum_{S \subseteq \Omega \setminus \{i, j\}} \frac{|S|! (n - |S| - 2)!}{(n - 1)!} (v(S \cup \{i, j\}) - v(S \cup \{j\}) - v(S \cup \{i\}) + v(S)). \end{aligned}$$

In Equation (13), the interaction is given as $\phi_{i,w/j} - \phi_{i,w/oj}$. Here, $\phi_{i,w/j}$ represents the specific game, in which the unit j is always present. In this case, we only need to consider the presence and absence of other $n - 1$ players, except for the unit j . $\phi_{i,w/oj}$ represents the specific game, in which the unit j is always absent. In this case, we also only need to consider the presence and absence of other $n - 1$ players, except for the unit j . $\phi_{i,w/j}$ and $\phi_{i,w/oj}$ are also implemented as Shapley values. When perturbation unit j is always present, the contribution of perturbation unit i is given as follows.

$$\phi_{i,w/j} = \sum_{S \subseteq \Omega \setminus \{i, j\}} \frac{|S|! (n - |S| - 2)!}{(n - 1)!} (v(S \cup \{i, j\}) - v(S \cup \{j\})).$$

In this game, because the perturbation unit j is always present, we can consider there are only $n - 1$ players.

When perturbation unit j is always absent, the contribution of perturbation unit i is given as follows.

$$\phi_{i,w/oj} = \sum_{S \subseteq \Omega \setminus \{i, j\}} \frac{|S|! (n - |S| - 2)!}{(n - 1)!} (v(S \cup \{i\}) - v(S)).$$

In this game, because the perturbation unit j is always absent, we can consider there are only $n - 1$ players.

In this way,

$$\begin{aligned} I'_{ij}(\delta) &= \phi_{i,w/j} - \phi_{i,w/oj} \\ &= \sum_{S \subseteq \Omega \setminus \{i, j\}} \frac{|S|! (n - |S| - 2)!}{(n - 1)!} (v(S \cup \{i, j\}) - v(S \cup \{j\}) - v(S \cup \{i\}) + v(S)). \end{aligned}$$

Therefore, we have

$$I_{ij}(\delta) = I'_{ij}(\delta).$$

□

E PROOF OF PROPOSITION 1

To simplify the problem setting, we do not consider some tricks in adversarial attacking, such as gradient normalization and the clip operation. In multi-step attacking, the final perturbation generated after t steps is given as follows.

$$\delta_{\text{multi}}^t \stackrel{\text{def}}{=} \alpha \sum_{t'=0}^{t-1} \nabla_x \ell(h(x + \delta_{\text{multi}}^{t'}), y),$$

where α represents the step size, and $\ell(h(x), y)$ is referred as the classification loss.

To simplify the notation, we use $g(x)$ to denote $\nabla_x \ell(h(x), y)$, i.e. $g(x) \stackrel{\text{def}}{=} \nabla_x \ell(h(x), y)$. Furthermore, we define the update of the perturbation with the multi-step attack at each step t as follows.

$$\Delta x_{\text{multi}}^t \stackrel{\text{def}}{=} \alpha \cdot g(x + \delta_{\text{multi}}^{t-1}). \quad (14)$$

In this way, the perturbation can be written as follows.

$$\delta_{\text{multi}}^t = \Delta x_{\text{multi}}^1 + \Delta x_{\text{multi}}^2 + \cdots + \Delta x_{\text{multi}}^{t-1}. \quad (15)$$

Lemma 1. *Given the sample $x \in \mathbb{R}^n$ and the adversarial perturbation $\delta \in \mathbb{R}^n$, we use $\Omega = \{1, 2, \dots, n\}$ to denote the set of all perturbation units. The score function is denoted by $v(S) = L(x + \delta^{(S)})$, where $\delta^{(S)}$ satisfies $\forall i \in S, \delta_i^{(S)} = \delta_i; \forall i \notin S, \delta_i^{(S)} = 0$. The Shapley interaction between perturbation units a, b can be written as $I_{ab} = \delta_a H_{ab}(x) \delta_b + \hat{R}_2(\delta)$, where $H_{ab}(x) = \frac{\partial^2 L(x)}{\partial x_a \partial x_b}$ represents the element of the Hessian matrix, and $\hat{R}_2(\delta)$ denotes terms with elements in δ of higher than the second order.*

Proof. The Shapley interaction between perturbation units a, b is

$$I_{ab}(\delta) = \sum_{S \subseteq \Omega \setminus \{a, b\}} \frac{|S|! (n - |S| - 2)!}{(n - 1)!} [v(S \cup \{a, b\}) - v(S \cup \{b\}) - v(S \cup \{a\}) + v(S)],$$

where $v(S) = L(x + \delta^{(S)})$. Here, the classification loss can be approximated as $L(x + \delta) = L(x) + g^T(x) \delta + \frac{1}{2} \delta^T H(x) \delta + R_2(\delta)$ using Taylor series. Thus, $\forall S' \subseteq \Omega$,

$$v(S') = L(x) + \sum_{a \in S'} g_a(x) \delta_a + \frac{1}{2} \sum_{a, b \in S'} \delta_a H_{ab}(x) \delta_b + R_2^{S'}(\delta).$$

where $R_2^{S'}(\delta)$ denotes terms with elements in $\delta^{(S')}$ of higher than the second order.

In this way, the Shapley interaction I_{ab} is given as

$$\begin{aligned} I_{ab}(\delta) &= \sum_{S \subseteq \Omega \setminus \{a, b\}} \frac{|S|! (n - |S| - 2)!}{(n - 1)!} [v(S \cup \{a, b\}) - v(S \cup \{b\}) - v(S \cup \{a\}) + v(S)] \\ &= \sum_{S \subseteq \Omega \setminus \{a, b\}} \frac{|S|! (n - |S| - 2)!}{(n - 1)!} \{ [L(x) + \sum_{a' \in S \cup \{a, b\}} g_{a'}(x) \delta_{a'} + \frac{1}{2} \sum_{a', b' \in S \cup \{a, b\}} \delta_{a'} H_{a'b'}(x) \delta_{b'} + R_2^{(S \cup \{a, b\})}(\delta)] \\ &\quad - [L(x) + \sum_{a' \in S \cup \{b\}} g_{a'}(x) \delta_{a'} + \frac{1}{2} \sum_{a', b' \in S \cup \{b\}} \delta_{a'} H_{a'b'}(x) \delta_{b'} + R_2^{(S \cup \{b\})}(\delta)] \\ &\quad - [L(x) + \sum_{a' \in S \cup \{a\}} g_{a'}(x) \delta_{a'} + \frac{1}{2} \sum_{a', b' \in S \cup \{a\}} \delta_{a'} H_{a'b'}(x) \delta_{b'} + R_2^{(S \cup \{a\})}(\delta)] \\ &\quad + L(x) + \sum_{a' \in S} g_{a'}(x) \delta_{a'} + \frac{1}{2} \sum_{a', b' \in S} \delta_{a'} H_{a'b'}(x) \delta_{b'} + R_2^{(S)}(\delta) \} \end{aligned}$$

$$\begin{aligned}
&= \sum_{S \subseteq \Omega \setminus \{a,b\}} \frac{|S|! (n - |S| - 2)!}{(n - 1)!} \{\delta_a H_{ab}(x) \delta_b\} \\
&+ \underbrace{\sum_{S \subseteq \Omega \setminus \{a,b\}} \frac{|S|! (n - |S| - 2)!}{(n - 1)!} [R_2^{(S \cup \{a,b\})}(\delta) - R_2^{(S \cup \{a\})}(\delta) - R_2^{(S \cup \{b\})}(\delta) + R_2^{(S)}(\delta)]}_{\hat{R}_2(\delta)} \\
&= \left\{ \sum_{s=0}^{n-2} \sum_{\substack{S \subseteq \Omega \setminus \{a,b\}, \\ |S|=s}} \frac{s! (n - s - 2)!}{(n - 1)!} [\delta_a H_{ab}(x) \delta_b] \right\} + \hat{R}_2(\delta) \\
&= \left\{ \sum_{s=0}^{n-2} \frac{(n - 2)!}{s! (n - s - 2)!} \frac{s! (n - s - 2)!}{(n - 1)!} [\delta_a H_{ab}(x) \delta_b] \right\} + \hat{R}_2(\delta) \\
&= \delta_a H_{ab}(x) \delta_b + \hat{R}_2(\delta),
\end{aligned}$$

where $\hat{R}_2(\delta)$ denotes terms with elements in δ of higher than the second order. \square

Lemma 2. The update of the perturbation with the multi-step attack at step t defined in Equation (14) can be written as $\Delta x_{\text{multi}}^t = \alpha [I + \alpha H(x)]^{t-1} g(x) + \hat{R}_1^t$, where $g(x) \stackrel{\text{def}}{=} \nabla_x \ell(h(x), y)$ represents the gradient, and $H(x) \stackrel{\text{def}}{=} \nabla_x^2 \ell(h(x), y)$ represents the Hessian matrix. \hat{R}_1^t denotes terms with elements in $\delta_{\text{multi}}^{t-1}$ of higher than the first order.

Proof. If $t = 1$, $\Delta x_{\text{multi}}^1 = \alpha \cdot g(x)$.

Let $\forall t' < t$, $\Delta x_{\text{multi}}^{t'} = \alpha [I + \alpha H(x)]^{t'-1} g(x) + \hat{R}_1^{t'}$, then we have

$$\begin{aligned}
\Delta x_{\text{multi}}^t &= \alpha \cdot g(x + \delta_{\text{multi}}^{t-1}) \quad // \quad \text{According to Equation (14)} \\
&= \alpha \cdot g(x + \Delta x_{\text{multi}}^1 + \Delta x_{\text{multi}}^2 + \cdots + \Delta x_{\text{multi}}^{t-1}) \quad // \quad \text{According to Equation (15)} \\
&= \alpha \cdot g \left(x + \alpha \left[I + [I + \alpha H(x)] + [I + \alpha H(x)]^2 + \cdots + [I + \alpha H(x)]^{t-2} \right] g(x) + \sum_{t'=1}^{t-1} \hat{R}_1^{t'} \right),
\end{aligned}$$

where $\hat{R}_1^{t'}$ denotes terms of elements in $\delta_{\text{multi}}^{t'-1}$ of higher than the first order.

Using the Taylor series, we get

$$\Delta x_{\text{multi}}^t = \alpha \cdot g(x) + \alpha^2 H(x) T(x) + \underbrace{\alpha H(x) \sum_{t'=1}^{t-1} \hat{R}_1^{t'}}_{\hat{R}_1^t} + R_1^{t-1}, \quad (16)$$

where R_1^{t-1} denotes terms with elements $\delta_{\text{multi}}^{t-1}$ of higher than the first order. $T(x)$ in Equation (16) is given as follows.

$$T(x) = \left[I + [I + \alpha H(x)] + [I + \alpha H(x)]^2 + \cdots + [I + \alpha H(x)]^{t-2} \right] g(x). \quad (17)$$

Multiply $(I + \alpha H(x))$ on both sides of Equation (17), and we get

$$(I + \alpha H(x)) T(x) = \alpha \cdot \left[[I + \alpha H(x)] + [I + \alpha H(x)]^2 + \cdots + [I + \alpha H(x)]^{t-1} \right] g(x). \quad (18)$$

Then, according to Equation (18) and Equation (17), we get

$$H(x) T(x) = \left[[I + \alpha H(x)]^{t-1} - I \right] g(x). \quad (19)$$

Substituting Equation (19) back to Equation (16), we have

$$\Delta x_{\text{multi}}^t = \alpha [I + \alpha H(x)]^{t-1} g(x) + \hat{R}_1^t.$$

In this way, we have proved that $\forall t \geq 1$, $\Delta x_{\text{multi}}^t = \alpha [I + \alpha H(x)]^{t-1} g(x) + \hat{R}_1^t$. \square

Proposition 1. Given an input sample $x \in \mathbb{R}^n$ and a DNN $h(\cdot)$ trained for classification, the adversarial perturbation generated by the multi-step attack via gradient descent is given as $\delta_{\text{multi}}^m = \alpha \sum_{t=0}^{m-1} \nabla_x \ell(h(x + \delta_{\text{multi}}^t), y)$, where δ_{multi}^t denotes the perturbation after the t -th step of updating, and m is referred to as the total number of steps. The adversarial perturbation generated by the single-step attack is given as $\delta_{\text{single}} = \alpha m \nabla_x \ell(h(x), y)$. The expectation of interactions between perturbation units in δ_{multi}^m , $\mathbb{E}_{a,b}[I_{ab}(\delta_{\text{multi}}^m)]$, is larger than $\mathbb{E}_{a,b}[I_{ab}(\delta_{\text{single}})]$, i.e. $\mathbb{E}_{a,b}[I_{ab}(\delta_{\text{multi}}^m)] \geq \mathbb{E}_{a,b}[I_{ab}(\delta_{\text{single}})]$.

E.1 FAIRNESS OF COMPARISONS OF INTERACTIONS INSIDE DIFFERENT PERTURBATIONS

Proposition 1 is valid for different loss functions of generating of adversarial perturbations. In this section, we discuss the fairness of comparisons of interactions inside different perturbations.

When we compare interactions inside different perturbations, magnitudes of these perturbations should be similar, because the comparison of interactions between adversarial perturbations of different magnitudes is not fair. For fair comparisons, in Section 3.1, this paper controls the magnitude of the single-step attack by setting the step size of the single-step attack as αm , where α and m denotes the step size and the total number of steps of the multi-step attack, respectively. The equivalent step size αm makes the magnitude of perturbations generated by the single-step attack to be similar to that of perturbations generated by the multi-step attack, when we use the target score before the softmax layer to generate adversarial perturbations, such as $\tilde{\ell}(h(x), y) = \max_{y' \neq y} h(x) - h_y(x)$. In this case, the magnitude of the gradient $\nabla_x \tilde{\ell}(h(x), y)$ is relatively stable. In particular, this type of loss has been widely used. For example, one of the most widely used attacking (Carlini & Wagner, 2017), uses the score before the softmax layer for targeted attacking.

E.2 PROOF OF PROPOSITION 1

Proof. According to Lemma 2, the update of the perturbation with the multi-step attack at the step t is given as follows.

$$\Delta x_{\text{multi}}^t = \alpha [I + \alpha H(x)]^{t-1} g(x) + \hat{R}_1^t, \quad (20)$$

where \hat{R}_1^t denotes terms with elements in $\delta_{\text{multi}}^{t-1}$ of higher than the first order, and α represents the step size.

To simplify the notation without causing ambiguity, we write $g(x)$ and $H(x)$ as g and H , respectively. In this way, according to Equation (15) and Equation (20), δ_{multi}^m can be written as follows.

$$\begin{aligned} \delta_{\text{multi}}^m &= \alpha \left[I + [I + \alpha H] + [I + \alpha H]^2 + \dots + [I + \alpha H]^{m-1} \right] g + \sum_{t=1}^m \hat{R}_1^t \\ &= \alpha \left[mI + \frac{\alpha m(m-1)}{2} H + \dots \right] g + \sum_{t=1}^m \hat{R}_1^t, \end{aligned} \quad (21)$$

where m represents the total number of steps. According to Lemma 1, the Shapley interaction between perturbation units a, b in δ_{multi}^m is given as follows.

$$I_{ab}(\delta_{\text{multi}}^m) = \delta_{\text{multi},a}^m H_{ab} \delta_{\text{multi},b}^m + \hat{R}_2(\delta_{\text{multi}}^m), \quad (22)$$

where $\hat{R}_2(\delta_{\text{multi}}^m)$ denotes terms with elements in δ_{multi}^m of higher than the second order.

According to Equation (21) and Equation (22), we have

$$\begin{aligned}
I_{ab}(\delta_{\text{multi}}^m) &= H_{ab} \left[\alpha m g_a + \frac{\alpha^2 m(m-1)}{2} \sum_{b'=1}^n (H_{ab'} g_{b'}) + \cdots + \sum_{t=1}^m \underbrace{o(\delta_{\text{multi},a}^t)}_{\substack{\text{terms of } \delta_{\text{multi},a}^t \\ \text{of higher than the first order,} \\ \text{which corresponds to the term of} \\ \hat{R}_1^t \text{ in Equation (21)}}} \right] \\
&\quad + \alpha m g_b + \frac{\alpha^2 m(m-1)}{2} \sum_{a'=1}^n (H_{a'b} g_{a'}) + \cdots + \underbrace{o(\delta_{\text{multi},b}^t)}_{\substack{\text{terms of } \delta_{\text{multi},b}^t \\ \text{of higher than the first order,} \\ \text{which corresponds to the term of} \\ \hat{R}_1^t \text{ in Equation (21)}}} \Big] + \hat{R}_2(\delta_{\text{multi}}^m) \\
&= \underbrace{\alpha^2 m^2 g_a g_b H_{ab}}_{\text{first-order terms w.r.t. elements in } H} \\
&\quad + \underbrace{\left[\frac{\alpha^3(m-1)m^2}{2} g_b \sum_{b'=1}^n (H_{ab'} g_{b'}) + \frac{\alpha^3(m-1)m^2}{2} g_a \sum_{a'=1}^n (H_{a'b} g_{a'}) \right] H_{ab}}_{\text{second-order terms w.r.t. elements in } H} \\
&\quad + \underbrace{\left[\frac{\alpha^4(m-1)^2 m^2}{4} \sum_{b'=1}^n (H_{ab'} g_{b'}) \sum_{a'=1}^n (H_{a'b} g_{a'}) H_{ab} + \dots \right]}_{\mathcal{R}_2^{\text{multi}}(H)} \\
&\quad + \underbrace{\left[\sum_{t=1}^m o(\delta_{\text{multi},a}^t) \right] H_{ab} \delta_{\text{multi},b}^m + \left[\sum_{t=1}^m o(\delta_{\text{multi},b}^t) \right] H_{ab} \delta_{\text{multi},a}^m}_{\hat{R}_2'(\delta_{\text{multi}}^m)} + \hat{R}_2(\delta_{\text{multi}}^m) \\
&= \alpha^2 m^2 g_a g_b H_{ab} + \frac{\alpha^3(m-1)m^2}{2} g_a H_{ab} \sum_{a'=1}^n (H_{a'b} g_{a'}) \\
&\quad + \frac{\alpha^3(m-1)m^2}{2} g_b H_{ab} \sum_{b'=1}^n (H_{ab'} g_{b'}) + \hat{R}_2'(\delta_{\text{multi}}^m) + \mathcal{R}_2^{\text{multi}}(H), \tag{23}
\end{aligned}$$

where $\mathcal{R}_2^{\text{multi}}(H)$ represents terms with elements in H of higher than the second order, and $\hat{R}_2'(\delta_{\text{multi}}^m)$ represents terms with elements in δ_{multi}^m of higher than the second order.

Let us consider the single-step attack. When we compare interactions inside different perturbations, magnitudes of these perturbations should be similar, because the comparison of interactions between adversarial perturbations of different magnitudes is not fair. For fair comparisons, in Section 3.1, this paper controls the magnitude of the single-step attack, as follows. The single-step attack only uses the gradient information on the original input x , which generates adversarial perturbations as:

$$\delta_{\text{single}} = \alpha m g.$$

Therefore, according to Lemma 1, the interaction between perturbation units a, b of δ_{single} is given as follows.

$$\begin{aligned}
I_{ab}(\delta_{\text{single}}) &= \delta_{\text{single},a} H_{ab} \delta_{\text{single},b} + \hat{R}_2(\delta_{\text{single}}) \\
&= m^2 \alpha^2 g_a g_b H_{ab} + \hat{R}_2(\delta_{\text{single}}), \tag{24}
\end{aligned}$$

where $\hat{R}_2(\delta_{\text{single}})$ denotes terms with elements in δ_{single} of higher than the second order. In this way, according to Equation (23) and Equation (24), the expectation of the difference between $I_{ab}(\delta_{\text{multi}}^m)$ and $I_{ab}(\delta_{\text{single}})$ is given as follows.

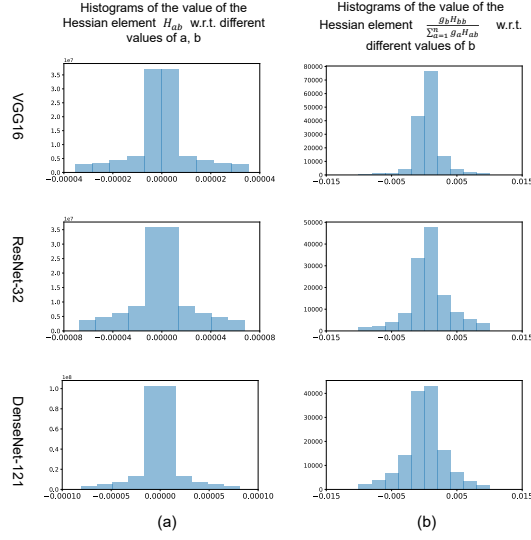


Figure 4: (a) Histograms of the value of the Hessian element $H_{ab}(x)$ w.r.t. different values of a, b . (b) Histograms of the value of $\frac{g_b H_{bb}}{\sum_{a=1}^n g_a H_{ab}}$ w.r.t. different values of b . Because the Hessian of the DNN with the ReLU activation is not well defined, we replace the ReLU activation with the Softplus activation $f(x) = \frac{1}{\beta} \log(1 + e^{-\beta x})$. We train VGG-16, ResNet-32, and DenseNet-121 on the CIFAR-10 dataset (Krizhevsky et al., 2009), and use the cross-entropy loss as the classification loss.

$$\begin{aligned}
& \mathbb{E}_{a,b} [I_{ab}(\delta_{\text{multi}}^m) - I_{ab}(\delta_{\text{single}})] \\
&= \mathbb{E}_{a,b} \left[\frac{\alpha^3(m-1)m^2}{2} g_a H_{ab} \sum_{a'=1}^n (H_{a'b} g_{a'}) + \frac{\alpha^3(m-1)m^2}{2} g_b H_{ab} \sum_{b'=1}^n (H_{ab'} g_{b'}) \right. \\
&\quad \left. + \hat{R}_2'(\delta_{\text{multi}}^m) + \mathcal{R}_2^{\text{multi}}(H) - \hat{R}_2(\delta_{\text{single}}) \right] \\
&= \frac{\alpha^3(m-1)m^2}{2} \mathbb{E}_{a,b} \left[\underbrace{g_a H_{ab} \sum_{a'=1}^n (H_{a'b} g_{a'})}_{U_{ab}} + \underbrace{g_b H_{ab} \sum_{b'=1}^n (H_{ab'} g_{b'})}_{U_{ba}} \right] + \mathbb{E}_{a,b} [R_{ab}],
\end{aligned}$$

where

$$R_{ab} = \hat{R}_2'(\delta_{\text{multi}}^m) + \mathcal{R}_2^{\text{multi}}(H) - \hat{R}_2(\delta_{\text{single}}).$$

Assumption 1: Magnitudes of elements in the Hessian matrix $H(x)$ is small that $|H_{ab}(x)| \ll 1$, where $1 \leq a, b \leq n$. Therefore, $H^k(x) \approx 0$, if $k > 2$.

We verify the assumption by directly measuring the value of $H_{ab}(x)$. As Fig. 4 (a) shows, the value of $H_{ab}(x)$ is very small that $|H_{ab}(x)| \ll 1$.

According to Assumption 1, we have $R_2^{\text{multi}}(H) \approx 0$. Note that the magnitude of δ_{multi}^m and the magnitude of δ_{single} are small, then $\hat{R}_2'(\delta_{\text{multi}}^m) \approx 0$, and $R_2(\delta_{\text{single}}) \approx 0$. In this way, we have $\mathbb{E}_{a,b}[R_{ab}] = \mathbb{E}_{a,b}[\hat{R}_2'(\delta_{\text{multi}}^m) + R_2(\delta_{\text{single}}) + R_2^{\text{multi}}(H)] \approx 0$.

Moreover, for the expectation of U_{ab} , we have

$$\mathbb{E}_{a,b}[U_{ab}] = \frac{1}{n(n-1)} \sum_{b=1}^n \sum_{a \neq b} g_a H_{ab} \sum_{a'=1}^n (g_{a'} H_{a'b})$$

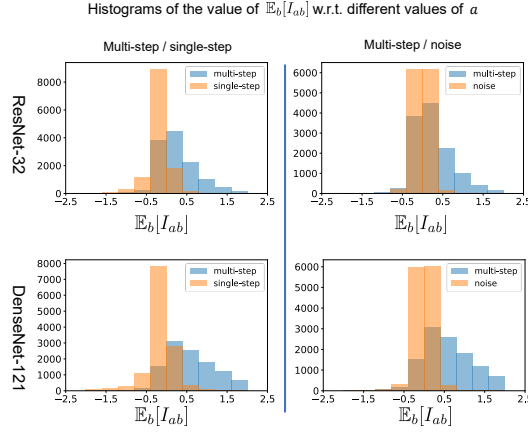


Figure 5: Histograms of the value of $\mathbb{E}_b[I_{ab}]$ w.r.t. different values of a

$$= \frac{1}{n(n-1)} \sum_{b=1}^n \left\{ \left[\underbrace{\left(\sum_{a=1}^n g_a H_{ab} \right)}_A - \underbrace{g_b H_{bb}}_B \right] \underbrace{\left(\sum_{a'=1}^n g_{a'} H_{a'b} \right)}_A \right\}$$

Let us focus on terms of A and B . Note that A is the sum of n terms (n is large). In comparisons, B is just a single term in A . Therefore, the sign of $A - B$ is usually dominated by the term A . In this way, we get $\text{Prob}[\text{sign}(A - B) = \text{sign}(A)] \approx 1$. Therefore, $\text{Prob}[(A - B)A \geq 0] \approx 1$. We verify this assumption by measuring the value of $\frac{g_b H_{bb}}{\sum_{a=1}^n g_a H_{ab}}$. If $\text{Prob}\left[\left|\frac{g_b H_{bb}}{\sum_{a=1}^n g_a H_{ab}}\right| \ll 1\right] \approx 1$, then we have $\text{Prob}[\text{sign}(A - B) = \text{sign}(A)] \approx 1$. As Fig. 4 (b) shows, the value of $\frac{g_b H_{bb}}{\sum_{a=1}^n g_a H_{ab}}$ is very small that $\left|\frac{g_b H_{bb}}{\sum_{a=1}^n g_a H_{ab}}\right| \ll 1$. To this end, we have $(A - B)B \geq 0$, and we get

$$\mathbb{E}_{a,b}[U_{ab}] \geq 0 \quad (25)$$

Due to the symmetry of a, b , we have $\mathbb{E}_{a,b}[U_{ba}] = \mathbb{E}_{a,b}[U_{ab}]$. Therefore,

$$\begin{aligned} & \mathbb{E}_{a,b}[I_{ab}(\delta_{\text{multi}}) - I_{ab}(\delta_{\text{single}})] \\ &= \frac{\alpha^3(m-1)m^2}{2} \mathbb{E}_{a,b}[U_{ab} + U_{ba}] + \mathbb{E}_{a,b}[R_{ab}] \\ &\approx \alpha^3(m-1)m^2 \mathbb{E}_{a,b}[U_{ab}] + 0 \\ &\geq 0. \end{aligned}$$

□

E.3 VERIFICATION OF PROPOSITION 1

We verify that perturbations generated by the multi-step attack tend to exhibit larger interaction than those generated by the single-step attack by measuring the value of $\mathbb{E}_b[I_{ab}]$. As shown in Appendix F, we prove that $\mathbb{E}_b[I_{ab}] = v(\Omega) - v(\Omega \setminus \{a\}) - v(\{a\}) + v(\emptyset)$. Because the image data is high-dimensional, the cost of computing $\mathbb{E}_b[I_{ab}]$ is high. As Appendix G demonstrates, given the input image, we can measure the interaction at the grid level, instead of the pixel level, to reduce the computational cost. Therefore, we divide the input image into 16×16 ($L = 16$) grids, and use Equation (28) to compute the interaction as $\mathbb{E}_{(p',q')} [I_{(p,q),(p',q')}(\delta)] = v(\Lambda) - v(\Lambda \setminus \{\Lambda_{pq}\}) - v(\{\Lambda_{pq}\}) + v(\emptyset)$, where (p, q) denotes the coordinate of a grid. The experiments were conducted with ImageNet validation images on ResNet-32 and DenseNet-121.

For fair comparisons, the magnitude of perturbations generated by the single-step attack is controlled to be same as that generated by the multi-step attack. As Figure 5 (left) shows, perturbations generated by the multi-step attack tend to exhibit larger interaction than those generated by the single-step attack.

E.4 PERTURBATIONS GENERATED BY THE MULTI-STEP ATTACK TEND TO EXHIBIT LARGER INTERACTION THAN GAUSSIAN NOISE

Moreover, we compare the interaction inside perturbation units generated by the multi-step attack with the Gaussian noise perturbation. Similarly, for fair comparisons, the magnitude of the Gaussian noise is controlled to be same as that generated by the multi-step attack. As Figure 5 (right) shows, perturbations generated by the multi-step attack tend to exhibit larger interaction than Gaussian noise.

F EXPECTATION OF THE SHAPLEY INTERACTION

In Equation (3), the Shapley interaction between two perturbation units i, j is given as follows.

$$I_{ij}(\delta) = \phi(S_{ij}|\Omega \setminus \{i, j\} \cup S_{ij}) - (\phi(i|\Omega \setminus \{j\}) + \phi(j|\Omega \setminus \{i\})),$$

where $\phi(S_{ij}|\Omega \setminus \{i, j\} \cup S_{ij})$ is the Shapley value of the singleton unit $S_{ij} = \{i, j\}$, when perturbation units i, j form a coalition. $\phi(i|\Omega \setminus \{j\})$ and $\phi(j|\Omega \setminus \{i\})$ are Shapley values of perturbation units i, j , when these two perturbation units work individually. In this way, we can write the Shapley interaction in a closed form as follows.

$$I_{ij}(\delta) = \sum_{S \subseteq \Omega \setminus \{i, j\}} \frac{|S|!(n - |S| - 2)!}{(n - 1)!} [v(S \cup \{i, j\}) - v(S \cup \{j\}) - v(S \cup \{i\}) + v(S)], \quad (26)$$

where $\forall S \subseteq \Omega, v(S) = \max_{y' \neq y} h_{y'}^{(s)}(x + \delta^{(S)}) - h_y^{(s)}(x + \delta^{(S)})$. The expectation of interaction is given as follows.

$$\mathbb{E}_{i,j} [I_{ij}(\delta)] = \frac{1}{n - 1} \mathbb{E}_i [v(\Omega) - v(\Omega \setminus \{i\}) - v(\{i\}) + v(\emptyset)], \quad (27)$$

which is proved as follows.

Proof. As proved in Appendix D, $I_{ij}(\delta) = I'_{ij}(\delta)$. Therefore, the interaction between players i and j is given as follows.

$$\begin{aligned} I_{ij}(\delta) &= \sum_{S \subseteq \Omega \setminus \{i, j\}} \frac{|S|!(n - |S| - 2)!}{(n - 1)!} [v(S \cup \{i, j\}) - v(S \cup \{j\})] - [v(S \cup \{i\}) - v(S)] \\ &= \phi_{j,w/i} - \phi_{j,w/o i}. \end{aligned}$$

The expectation of the interaction can be written as follows.

$$\mathbb{E}_{i,j} [I_{ij}(\delta)] = \frac{1}{(n - 1)} \mathbb{E}_i \left\{ \sum_{j \in \Omega \setminus \{i\}} [\phi_{j,w/i} - \phi_{j,w/o i}] \right\}.$$

According to the **efficiency property** of Shapley values (please refer to Appendix A for details):

$$\begin{aligned} \sum_{j \in \Omega \setminus \{i\}} \phi_{j,w/i} &= v(\Omega) - v(\{i\}) \\ \sum_{j \in \Omega \setminus \{i\}} \phi_{j,w/o i} &= v(\Omega \setminus \{i\}) - v(\emptyset). \end{aligned}$$

In this way,

$$\mathbb{E}_{i,j} [I_{ij}(\delta)] = \frac{1}{n - 1} \mathbb{E}_i [v(\Omega) - v(\Omega \setminus \{i\}) - v(\{i\}) + v(\emptyset)].$$

□

G GRID-LEVEL INTERACTIONS FOR IMAGE DATA

Although the computation of $\mathbb{E}_{i,j}[I_{ij}(\delta)]$ can be simplified using Equation (27), the computational cost of $\mathbb{E}_{i,j}[I_{ij}(\delta)]$ is still high. Therefore, as Figure 6 shows, using the local property of images (Chen et al., 2018a), we can divide the entire image into $L \times L$ grids, and compute interactions at the grid level, instead of the pixel level. Let $\Lambda = \{\Lambda_{11}, \Lambda_{12}, \dots, \Lambda_{LL}\}$ denote the set of grids. We use (p, q) to denote the coordinate of a grid. In this way, the expectation of interactions between perturbation grids is given as follows.

$$\mathbb{E}_{(p,q),(p',q')} [I_{(p,q),(p',q')}(\delta)] = \frac{1}{L^2 - 1} \mathbb{E}_{(p,q)} [v(\Lambda) - v(\Lambda \setminus \{\Lambda_{pq}\}) - v(\{\Lambda_{pq}\}) + v(\emptyset)], \quad (28)$$

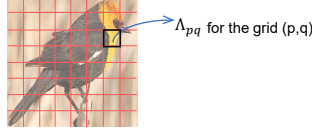


Figure 6: For the input image, we can divide the image into grids, and compute interactions at the grid level.

H DETAILS OF OBSERVING THE NEGATIVE CORRELATION BETWEEN THE TRANSFERABILITY AND THE INTERACTION

In Section 3.2, we directly measure the transfer utility and interactions of different adversarial perturbations. Here, we give more details of the experiments. We measure the transfer utility as $\text{Transfer Utility} = [\max_{y' \neq y} h_{y'}^{(t)}(x + \delta) - h_y^{(t)}(x + \delta)] - [\max_{y' \neq y} h_{y'}^{(t)}(x) - h_y^{(t)}(x)]$. We measure the interaction as $\mathbb{E}_{i,j}[I_{ij}(\delta)] = \frac{1}{n-1} \mathbb{E}_i [v(\Omega) - v(\Omega \setminus \{i\}) - v(\{i\}) + v(\emptyset)]$. As Appendix G demonstrates, to reduce the computational cost, given the input image, we can measure the interaction at the grid level, instead of the pixel level. Therefore, we divide the input image into 16×16 ($L = 16$) grids, and use Equation (28) to compute the interaction as $\mathbb{E}_{(p,q),(p',q')} [I_{(p,q),(p',q')}(\delta)] = \frac{1}{L^2 - 1} \mathbb{E}_{(p,q)} [v(\Lambda) - v(\Lambda \setminus \{\Lambda_{pq}\}) - v(\{\Lambda_{pq}\}) + v(\emptyset)]$, where (p, q) denotes the coordinate of a grid.

Using the validation set of the ImageNet dataset (Russakovsky et al., 2015), we generate adversarial perturbations on four types of DNNs, including ResNet-34/152(RN-34/152) (He et al., 2016) and DenseNet-121/201(DN-121/201) (Huang et al., 2017). We transfer adversarial perturbations generated on each ResNet to DenseNets. Similarly, we also transfer adversarial perturbations generated on each DenseNet to ResNets. Given an input image x , adversarial perturbations are generated using Equation (8), i.e. $\min_{\delta} -\ell(h(x + \delta), y) + c \cdot \|\delta\|_p^p$ s.t. $x + \delta \in [0, 1]^n$, where $c \in \mathbb{R}$ is a scalar constant. In this way, we gradually change the value of c as different hyper-parameters to generate different adversarial perturbations. For fair comparisons, we need to ensure adversarial perturbations generated with different hyper-parameters c to be comparable with each other. Thus, we select a constant τ and let $\|\delta\|_2 = \tau$ as the stopping criteria of all adversarial attacks. We set the number of steps as 1000. The threshold τ is set to ensure that attacks with different hyper-parameters τ are almost converged when the L_2 norm of the perturbation $\|\delta\|_2$ reaches τ .

I PROOF OF PROPOSITION 2

To simplify the problem setting, we do not consider some tricks in adversarial attacking, such as gradient normalization and the clip operation. In VR attack (Wu et al., 2018), the final perturbation generated after t steps is given as follows.

$$\delta_{\text{vr}}^t \stackrel{\text{def}}{=} \alpha \sum_{t'=0}^{t-1} \nabla_x \hat{\ell}(h(x + \delta_{\text{vr}}^{t'}), y),$$

where

$$\hat{\ell}(h(x), y) = \mathbb{E}_{\xi \sim \mathcal{N}(0, \sigma^2 I)} [\ell(h(x + \xi), y)]. \quad (29)$$

According to Equation (29), the gradient and the Hessian matrix of $\hat{\ell}(h(x), y)$ is given as follows.

$$\begin{aligned} \hat{g}(x) &= \nabla_x \hat{\ell}(h(x), y) \\ &= \mathbb{E}_{\xi \sim \mathcal{N}(0, \sigma^2 I)} [\nabla_x \ell(h(x + \xi), y)], \\ \hat{H}(x) &= \nabla_x^2 \hat{\ell}(h(x), y) \\ &= \mathbb{E}_{\xi \sim \mathcal{N}(0, \sigma^2 I)} [\nabla_x^2 \ell(h(x + \xi), y)]. \end{aligned} \quad (30)$$

where α represents the step size.

Lemma 3. *Given the Gaussian smoothed loss $\hat{\ell}(x) = \mathbb{E}_{\xi \sim \mathcal{N}(0, \sigma^2 I)} [\ell(h(x), y)]$, where $\ell(h(x), y)$ is the original classification loss, $\forall a \neq b, \forall c \neq a$, we have $\mathbb{E}_x [\hat{g}_a^2(x) \hat{H}_{ab}^2(x) - g_a^2(x) H_{ab}^2(x)] \leq 0$, $\mathbb{E}_x [\hat{g}_a(x) \hat{g}_b(x) \hat{H}_{ab}(x) - g_a(x) g_b(x) H_{ab}(x)] = 0$, and $\mathbb{E}_x [\hat{g}_a(x) \hat{g}_c(x) \hat{H}_{ab}(x) \hat{H}_{cb}(x) - g_a(x) g_c(x) H_{ab}(x) H_{cb}(x)] = 0$.*

Proof. According to Equation (30), we have

$$\begin{aligned} \hat{g}_a(x) &= \mathbb{E}_{\xi \sim \mathcal{N}(0, \sigma^2 I)} [g_a(x + \xi)] = \mathbb{E}_{x' \sim \mathcal{N}(x, \sigma^2 I)} [g_a(x')], \\ \hat{H}_{ab}(x) &= \mathbb{E}_{\xi \sim \mathcal{N}(0, \sigma^2 I)} \left[\frac{\partial g_a(x + \xi)}{\partial x_b} \right] = \mathbb{E}_{x' \sim \mathcal{N}(x, \sigma^2 I)} \left[\frac{\partial g_a(x')}{\partial x_b} \right] = \mathbb{E}_{x' \sim \mathcal{N}(x, \sigma^2 I)} [H_{ab}(x')]. \end{aligned}$$

This indicates that the gradient and the Hessian matrix in the VR attack are both smoothed by the Gaussian noise. Because the Lipschitz constants of $g_a(x)$ and $H_{ab}(x)$ are usually limited to a certain range, we can ignore the tiny probability of large gradients and large elements in the Hessian matrix, and roughly assume that $g_a(x) \sim \mathcal{N}(\hat{g}_a(x), \sigma_{g_a}^2)$, and $H_{ab}(x) \sim \mathcal{N}(\hat{H}_{ab}(x), \sigma_{H_{ab}}^2)$, where $\sigma_{g_a}, \sigma_{H_{ab}} \in \mathbb{R}$ are tow constants denoting the standard deviation. Thus, $g_a(x)$ and $H_{ab}(x)$ can be written as follows.

$$\begin{aligned} g_a(x) &= \hat{g}_a(x) + \epsilon_{g_a}, \quad \epsilon_{g_a} \sim \mathcal{N}(0, \sigma_{g_a}^2), \\ H_{ab}(x) &= \hat{H}_{ab}(x) + \epsilon_{H_{ab}}, \quad \epsilon_{H_{ab}} \sim \mathcal{N}(0, \sigma_{H_{ab}}^2). \end{aligned} \quad (31)$$

To simplify the notation without causing ambiguity, we write $\hat{g}(x)$ and $\hat{H}(x)$ as \hat{g} and \hat{H} , respectively. Moreover, we write $g(x)$ and $H(x)$ as g and H , respectively. In this way, we have

$$\begin{aligned} &\mathbb{E}_x [\hat{g}_a^2 \hat{H}_{ab}^2 - g_a^2 H_{ab}^2] \\ &= \mathbb{E}_x \mathbb{E}_{\epsilon_{g_a}, \epsilon_{H_{ab}}} [\hat{g}_a^2 \hat{H}_{ab}^2 - (\hat{g}_a + \epsilon_{g_a})^2 (\hat{H}_{ab} + \epsilon_{H_{ab}})^2] \\ &= -\mathbb{E}_x \mathbb{E}_{\epsilon_{g_a}, \epsilon_{H_{ab}}} [\epsilon_{g_a}^2 \hat{H}_{ab}^2 + \epsilon_{H_{ab}}^2 (\hat{g}_a + \epsilon_{g_a})^2 + 2\epsilon_{g_a} \hat{g}_a \hat{H}_{ab} + 2\epsilon_{H_{ab}} \hat{H}_{ab} (\hat{g}_a + \epsilon_{g_a})^2] \\ &\leq -\mathbb{E}_x \mathbb{E}_{\epsilon_{g_a}, \epsilon_{H_{ab}}} [2\epsilon_{g_a} \hat{g}_a \hat{H}_{ab} + 2\epsilon_{H_{ab}} \hat{H}_{ab} (\hat{g}_a + \epsilon_{g_a})^2] \\ &= -\mathbb{E}_x \left\{ \mathbb{E}_{\epsilon_{g_a}} [\epsilon_{g_a}] 2\hat{g}_a \hat{H}_{ab} + \mathbb{E}_{\epsilon_{g_a}} \left[\mathbb{E}_{\epsilon_{H_{ab}}} [\epsilon_{H_{ab}}] 2\hat{H}_{ab} (\hat{g}_a + \epsilon_{g_a})^2 \right] \right\} \\ &= -\mathbb{E}_x \left\{ 0 \cdot 2\hat{g}_a \hat{H}_{ab} + \mathbb{E}_{\epsilon_{g_a}} \left[0 \cdot 2\hat{H}_{ab} (\hat{g}_a + \epsilon_{g_a})^2 \right] \right\} \\ &= 0. \end{aligned}$$

According to Equation (31), we have $g_a = \hat{g}_a + \epsilon_{g_a}$, $g_b = \hat{g}_b + \epsilon_{g_b}$. Thus, we have

$$\begin{aligned} &\mathbb{E}_x [\hat{g}_a \hat{g}_b \hat{H}_{ab} - g_a g_b H_{ab}] \\ &= \mathbb{E}_x [\hat{g}_a(x) \hat{g}_b(x) \hat{H}_{ab} - (\hat{g}_a + \epsilon_{g_a})(\hat{g}_b + \epsilon_{g_b})(\hat{H}_{ab} + \epsilon_{H_{ab}})] \end{aligned}$$

$$\begin{aligned}
&= -\mathbb{E}_{x, \epsilon_{g_a}, \epsilon_{g_b}, \epsilon_{H_{ab}}} \left[\epsilon_{g_a} \epsilon_{g_b} \epsilon_H + \epsilon_{g_a} \epsilon_{g_b} \hat{H}_{ab} + \epsilon_{g_b} \epsilon_{H_{ab}} \hat{g}_a \right. \\
&\quad \left. + \epsilon_{H_{ab}} \epsilon_{g_a} \hat{g}_b + \epsilon_{g_b} \hat{g}_b \hat{H}_{ab} + \epsilon_{g_b} \hat{g}_a \hat{H}_{ab} + \epsilon_{H_{ab}} \hat{g}_a \hat{g}_b \right] \\
&= -\mathbb{E}_x \left[\mathbb{E}_{\epsilon_{g_a}} [\epsilon_{g_a}] \mathbb{E}_{\epsilon_{g_b}} [\epsilon_{g_b}] \mathbb{E}_{\epsilon_{H_{ab}}} [\epsilon_H] + \mathbb{E}_{\epsilon_{g_a}} [\epsilon_{g_a}] \mathbb{E}_{\epsilon_{g_b}} [\epsilon_{g_b}] \hat{H}_{ab} + \mathbb{E}_{\epsilon_{g_b}} [\epsilon_{g_b}] \mathbb{E}_{\epsilon_{H_{ab}}} [\epsilon_{H_{ab}}] \hat{g}_a \right. \\
&\quad \left. + \mathbb{E}_{\epsilon_{H_{ab}}} [\epsilon_{H_{ab}}] \mathbb{E}_{\epsilon_{g_a}} [\epsilon_{g_a}] \hat{g}_b + \mathbb{E}_{\epsilon_{g_a}} [\epsilon_{g_a}] \hat{g}_b \hat{H}_{ab} + \mathbb{E}_{\epsilon_{g_b}} [\epsilon_{g_b}] \hat{g}_a \hat{H}_{ab} + \mathbb{E}_{\epsilon_{H_{ab}}} [\epsilon_{H_{ab}}] \hat{g}_a \hat{g}_b \right] \\
&= -\mathbb{E}_x \left[0 \cdot 0 \cdot 0 + 0 \cdot 0 \cdot \hat{H}_{ab} + 0 \cdot 0 \cdot \hat{g}_a + 0 \cdot 0 \cdot \hat{g}_b + 0 \cdot \hat{g}_b \hat{H}_{ab} + 0 \cdot \hat{g}_a \hat{H}_{ab} + 0 \cdot \hat{g}_a \hat{g}_b \right] \\
&= 0.
\end{aligned}$$

Moreover, according to Equation (31), we have

$$\begin{aligned}
&\mathbb{E}_x \left[\hat{g}_a \hat{g}_c \hat{H}_{ab} \hat{H}_{cb} - g_a g_c H_{ab} H_{cb} \right] \\
&= \mathbb{E}_{x, \epsilon_{g_a}, \epsilon_{g_c}, \epsilon_{H_{ab}}, \epsilon_{H_{cb}}} \left[\hat{g}_a \hat{g}_c \hat{H}_{ab} \hat{H}_{cb} - (\hat{g}_a + \epsilon_{g_a})(\hat{g}_c + \epsilon_{g_c})(\hat{H}_{ab} + \epsilon_{H_{ab}})(\hat{H}_{cb} + \epsilon_{H_{cb}}) \right] \\
&= -\mathbb{E}_{x, \epsilon_{g_a}, \epsilon_{g_c}, \epsilon_{H_{ab}}, \epsilon_{H_{cb}}} \left[\epsilon_{g_a} \epsilon_{g_c} \epsilon_{H_{ab}} \epsilon_{H_{cb}} \right. \\
&\quad + \epsilon_{g_c} \epsilon_{H_{ab}} \epsilon_{H_{cb}} \hat{g}_a + \epsilon_{g_a} \epsilon_{H_{ab}} \epsilon_{H_{cb}} \hat{g}_c + \epsilon_{g_a} \epsilon_{g_c} \epsilon_{H_{cb}} \hat{H}_{ab} + \epsilon_{g_a} \epsilon_{g_c} \epsilon_{H_{ab}} \hat{H}_{cb} \\
&\quad + \epsilon_{g_a} \epsilon_{g_c} \hat{H}_{ab} \hat{H}_{cb} + \epsilon_{g_a} \epsilon_{H_{ab}} \hat{g}_c \hat{H}_{cb} + \epsilon_{g_a} \epsilon_{H_{cb}} \hat{g}_c \hat{H}_{ab} \\
&\quad + \epsilon_{g_c} \epsilon_{H_{ab}} \hat{g}_a \hat{H}_{cb} + \epsilon_{g_c} \epsilon_{H_{cb}} \hat{g}_a \hat{H}_{ab} + \epsilon_{H_{ab}} \epsilon_{H_{cb}} \hat{g}_a \hat{g}_c \\
&\quad \left. + \epsilon_{g_a} \hat{g}_c \hat{H}_{ab} \hat{H}_{cb} + \epsilon_{g_c} \hat{g}_a \hat{H}_{ab} \hat{H}_{cb} + \epsilon_{H_{ab}} \hat{g}_a \hat{g}_c \hat{H}_{cb} + \epsilon_{H_{cb}} \hat{g}_a \hat{g}_c \hat{H}_{ab} \right] \\
&= -\mathbb{E}_x \left[\mathbb{E}_{\epsilon_{g_a}} [\epsilon_{g_a}] \mathbb{E}_{\epsilon_{g_c}} [\epsilon_{g_c}] \mathbb{E}_{\epsilon_{H_{ab}}} [\epsilon_{H_{ab}}] \mathbb{E}_{\epsilon_{H_{cb}}} [\epsilon_{H_{cb}}] + \mathbb{E}_{\epsilon_{g_c}} [\epsilon_{g_c}] \mathbb{E}_{\epsilon_{H_{ab}}} [\epsilon_{H_{ab}}] \mathbb{E}_{\epsilon_{H_{cb}}} [\epsilon_{H_{cb}}] \hat{g}_a \right. \\
&\quad + \mathbb{E}_{\epsilon_{g_a}} [\epsilon_{g_a}] \mathbb{E}_{\epsilon_{H_{ab}}} [\epsilon_{H_{ab}}] \mathbb{E}_{\epsilon_{H_{cb}}} [\epsilon_{H_{cb}}] \hat{g}_c + \mathbb{E}_{\epsilon_{g_a}} [\epsilon_{g_a}] \mathbb{E}_{\epsilon_{g_c}} [\epsilon_{g_c}] \mathbb{E}_{\epsilon_{H_{cb}}} [\epsilon_{H_{cb}}] \hat{H}_{ab} \\
&\quad + \mathbb{E}_{\epsilon_{g_a}} [\epsilon_{g_a}] \mathbb{E}_{\epsilon_{g_c}} [\epsilon_{g_c}] \mathbb{E}_{\epsilon_{H_{ab}}} [\epsilon_{H_{ab}}] \hat{H}_{cb} \\
&\quad + \mathbb{E}_{\epsilon_{g_a}} [\epsilon_{g_a}] \mathbb{E}_{\epsilon_{g_c}} [\epsilon_{g_c}] \hat{H}_{ab} \hat{H}_{cb} + \mathbb{E}_{\epsilon_{g_a}} [\epsilon_{g_a}] \mathbb{E}_{\epsilon_{H_{ab}}} \epsilon_{H_{ab}} \hat{g}_c \hat{H}_{cb} + \mathbb{E}_{\epsilon_{g_a}} [\epsilon_{g_a}] \mathbb{E}_{\epsilon_{H_{cb}}} [\epsilon_{H_{cb}}] \hat{g}_c \hat{H}_{ab} \\
&\quad + \mathbb{E}_{\epsilon_{g_c}} [\epsilon_{g_c}] \mathbb{E}_{\epsilon_{H_{ab}}} [\epsilon_{H_{ab}}] \hat{g}_a \hat{H}_{cb} + \mathbb{E}_{\epsilon_{g_c}} [\epsilon_{g_c}] \mathbb{E}_{\epsilon_{H_{cb}}} [\epsilon_{H_{cb}}] \hat{g}_a \hat{H}_{ab} + \mathbb{E}_{\epsilon_{H_{ab}}} [\epsilon_{H_{ab}}] \mathbb{E}_{\epsilon_{H_{cb}}} [\epsilon_{H_{cb}}] \hat{g}_a \hat{g}_c \\
&\quad \left. + \mathbb{E}_{\epsilon_{g_a}} [\epsilon_{g_a}] \hat{g}_c \hat{H}_{ab} \hat{H}_{cb} + \mathbb{E}_{\epsilon_{g_c}} [\epsilon_{g_c}] \hat{g}_a \hat{H}_{ab} \hat{H}_{cb} + \mathbb{E}_{\epsilon_{H_{ab}}} [\epsilon_{H_{ab}}] \hat{g}_a \hat{g}_c \hat{H}_{cb} + \mathbb{E}_{\epsilon_{H_{cb}}} [\epsilon_{H_{cb}}] \hat{g}_a \hat{g}_c \hat{H}_{ab} \right] \\
&= -\mathbb{E}_x \left[0 + 0 \cdot \hat{g}_a + 0 \cdot \hat{g}_c + 0 \cdot \hat{H}_{ab} + 0 \cdot \hat{H}_{cb} \right. \\
&\quad + 0 \cdot \hat{H}_{ab} \hat{H}_{cb} + 0 \cdot \hat{g}_c \hat{H}_{cb} + 0 \cdot \hat{g}_c \hat{H}_{ab} + 0 \cdot \hat{g}_a \hat{H}_{cb} + 0 \cdot \hat{g}_a \hat{H}_{ab} + 0 \cdot \hat{g}_a \hat{g}_c \\
&\quad \left. + 0 \cdot \hat{g}_c \hat{H}_{ab} \hat{H}_{cb} + 0 \cdot \hat{g}_a \hat{H}_{ab} \hat{H}_{cb} + 0 \cdot \hat{g}_a \hat{g}_c \hat{H}_{cb} + 0 \cdot \hat{g}_a \hat{g}_c \hat{H}_{ab} \right] \\
&= 0.
\end{aligned}$$

□

Proposition 2. Given an input image $x \in \mathbb{R}^n$ and a DNN $h(\cdot)$ trained for classification, the adversarial perturbation generated by multi-step attack is denoted by $\delta_{\text{multi}}^m = \alpha \sum_{t=0}^{m-1} \nabla_x \ell(h(x + \delta_{\text{multi}}^t), y)$. The adversarial perturbation generated by VR Attack is denoted by $\delta_{\text{vr}}^m = \alpha \sum_{t=0}^{m-1} \nabla_x \hat{\ell}(h(x + \delta_{\text{vr}}^t), y)$, where $\hat{\ell}(h(x + \delta_{\text{vr}}^t), y) = \mathbb{E}_{\xi \sim \mathcal{N}(0, \sigma^2 I)} [\ell(h(x + \delta_{\text{vr}}^t + \xi), y)]$. Perturbation units of δ_{vr}^m tend to exhibit smaller interaction than δ_{multi}^m , i.e. $\mathbb{E}_x \mathbb{E}_{a, b} [I_{ab}(\delta_{\text{vr}}^m)] \leq \mathbb{E}_x \mathbb{E}_{a, b} [I_{ab}(\delta_{\text{multi}}^m)]$.

Proof. To simplify the notation without causing ambiguity, we write $\hat{g}(x)$ and $\hat{H}(x)$ as \hat{g} and \hat{H} , respectively. Moreover, we write $g(x)$ and $H(x)$ as g and H , respectively.

Just like the conclusion in Equation (23), we can write the interaction between $\delta_{\text{vr},a}^m$ and $\delta_{\text{vr},b}^m$ as follows.

$$\begin{aligned} I_{ab}(\delta_{\text{vr}}^m) &= \alpha^2 m^2 \hat{g}_a \hat{g}_b \hat{H}_{ab} + \frac{\alpha^3(m-1)m^2}{2} \hat{g}_a \hat{H}_{ab} \sum_{a'=1}^n (\hat{H}_{a'b} \hat{g}_{a'}) \\ &\quad + \frac{\alpha^3(m-1)m^2}{2} \hat{g}_b \hat{H}_{ab} \sum_{b'=1}^n (\hat{H}_{ab'} \hat{g}_{b'}) + \hat{R}_2^{\text{vr}}(\delta_{\text{vr}}^m) + \mathcal{R}_2^{\text{vr}}(\hat{H}), \end{aligned} \quad (32)$$

where α denotes the step size, and m denotes the total number of steps. To enable fair comparisons, we use the same step size α and number of steps m as multi-step attack to make the magnitude of δ_{vr} match the magnitude of δ_{multi} . $\mathcal{R}_2^{\text{vr}}(\hat{H})$ represents terms with elements in \hat{H} of higher than the second order, and $\hat{R}_2^{\text{vr}}(\delta_{\text{vr}}^m)$ represents terms with elements in δ_{vr}^m of higher than the second order.

In this way, according to Equation (32) and Equation (23), the expectation of the difference between $I_{ab}(\delta_{\text{vr}}^m)$ and $I_{ab}(\delta_{\text{multi}}^m)$ is given as follows.

$$\begin{aligned} &\mathbb{E}_x \mathbb{E}_{a,b} [I_{ab}(\delta_{\text{vr}}) - I_{ab}(\delta_{\text{multi}})] \\ &= \frac{\alpha^3(m-1)m^2}{2} \mathbb{E}_{a,b} \left\{ \mathbb{E}_x \left[\left[\hat{g}_a^2 \hat{H}_{ab}^2 - g_a^2 H_{ab}^2 \right] + \left[\hat{g}_b^2 \hat{H}_{ab}^2 - g_b^2 H_{ab}^2 \right] \right] \right\} + \mathbb{E}_{a,b} \mathbb{E}_x [R_{ab}^{\text{vr}}], \end{aligned}$$

where

$$\begin{aligned} R_{ab}^{\text{vr}} &= \frac{\alpha^3(m-1)m^2}{2} \left[\underbrace{\sum_{a' \in \{1,2,\dots,n\} \setminus \{a\}} \left[(\hat{g}_a \hat{g}_{a'} \hat{H}_{ab} \hat{H}_{a'b} - g_a g_{a'} H_{ab} H_{a'b}) \right]}_{V_{ab}} \right. \\ &\quad \left. + \underbrace{\sum_{b' \in \{1,2,\dots,n\} \setminus \{b\}} \left[(\hat{g}_b \hat{g}_{b'} \hat{H}_{ab} \hat{H}_{ab'} - g_b g_{b'} H_{ab} H_{ab'}) \right]}_{V_{ba}} \right] \\ &\quad + \alpha^2 m^2 \left[\hat{g}_a \hat{g}_b \hat{H}_{ab} - g_a g_b H_{ab} \right] + \hat{R}_2^{\text{vr}}(\delta_{\text{vr}}^m) - \hat{R}_2'(\delta_{\text{multi}}^m) + \mathcal{R}_2^{\text{vr}}(H) - R_2^{\text{multi}}(H) \end{aligned}$$

The expectation of R_{ab}^{vr} is give as follows.

$$\begin{aligned} &\mathbb{E}_x \mathbb{E}_{a,b} [R_{ab}^{\text{vr}}] \\ &= \frac{\alpha^3(m-1)m^2}{2} \left\{ \mathbb{E}_{a,b} \left[\mathbb{E}_x [V_{ab}] + \mathbb{E}_x [V_{ba}] + \frac{2}{\alpha(m-1)} \mathbb{E}_x \left[\hat{g}_a \hat{g}_b \hat{H}_{ab} - g_a g_b H_{ab} \right] \right] \right\} \\ &\quad + \mathbb{E}_x \mathbb{E}_{a,b} [\hat{R}_2^{\text{vr}}(\delta_{\text{vr}}^m) - \hat{R}_2'(\delta_{\text{multi}}^m) + R_2^{\text{vr}}(H) - R_2^{\text{multi}}(H)] \approx 0. \end{aligned}$$

According to Assumption 1, we have $R_2^{\text{vr}}(H) \approx 0$, and $R_2^{\text{multi}}(H) \approx 0$. Note that the magnitude of δ_{mi}^m and the magnitude of δ_{multi} are small, then $\hat{R}_2'(\delta_{\text{vr}}^m) \approx 0$, and $R_2(\delta_{\text{multi}}^m) \approx 0$. According to Lemma 3, we have $\mathbb{E}_x [\hat{g}_a \hat{g}_b \hat{H}_{ab} - g_a g_b H_{ab}] = 0$, $\mathbb{E}_x [\hat{g}_a \hat{g}_{a'} \hat{H}_{ab} \hat{H}_{a'b} - g_a g_{a'} H_{ab} H_{a'b}] = 0$. Therefore, we get $\mathbb{E}_x [V_{ab}] = 0$. In this way, $\mathbb{E}_x \mathbb{E}_{a,b} [R_{ab}^{\text{vr}}] \approx 0$.

Furthermore, according to Lemma 3, we have $\mathbb{E}_x [\hat{g}_a^2 \hat{H}_{ab}^2] - \mathbb{E}_x [g_a^2 H_{ab}^2] \leq 0$.

Therefore,

$$\begin{aligned} &\mathbb{E}_x \mathbb{E}_{a,b} [I_{ab}(\delta_{\text{vr}}) - I_{ab}(\delta_{\text{multi}})] \\ &= \frac{\alpha^3(m-1)m^2}{2} \mathbb{E}_{a,b} \left\{ \mathbb{E}_x \left[\hat{g}_a^2 \hat{H}_{ab}^2 - g_a^2 H_{ab}^2 \right] + \mathbb{E}_x \left[\hat{g}_b^2 \hat{H}_{ab}^2 - g_b^2 H_{ab}^2 \right] \right\} + \mathbb{E}_x \mathbb{E}_{a,b} [R_{ab}^{\text{vr}}] \end{aligned}$$

$$\begin{aligned} &\approx \frac{\alpha^3(m-1)m^2}{2} \mathbb{E}_{a,b} \left\{ \mathbb{E}_x \left[\hat{g}_a^2 \hat{H}_{ab}^2 - g_a^2 H_{ab}^2 \right] + \mathbb{E}_x \left[\hat{g}_b^2 \hat{H}_{ab}^2 - g_b^2 H_{ab}^2 \right] \right\} + 0 \\ &\leq 0 \end{aligned}$$

□

J PROOF OF PROPOSITION 3

To simplify the problem setting, we do not consider some tricks in adversarial attacking, such as gradient normalization and the clip operation. Note that the original MI Attack and the multi-step attack cannot be directly compared, since that magnitudes of the generated perturbations cannot be fairly controlled. The value of interactions is sensitive to the magnitude of perturbations. Comparing perturbations with different magnitudes is not fair. Thus, we slightly revise the MI Attack as

$$g_{\text{mi}}^t \stackrel{\text{def}}{=} \mu g_{\text{mi}}^{t-1} + (1 - \mu) \nabla_x \ell(h(x + \delta_{\text{mi}}^{t-1}), y), \quad (33)$$

where t denotes the step and $\mu = (t-1)/t$. $\ell(h(x), y)$ is referred as the classification loss. To simplify the notation, we use $g(x)$ to denote $\nabla_x \ell(h(x), y)$, i.e. $g(x) \stackrel{\text{def}}{=} \nabla_x \ell(h(x), y)$.

In MI attack, the final perturbation generated after t steps is given as follows.

$$\delta_{\text{mi}}^t \stackrel{\text{def}}{=} \alpha \sum_{t'=0}^{t-1} g_{\text{mi}}^{t'},$$

where α represents the step size.

Furthermore, we define the update of perturbation with the MI attack at each step t as follows.

$$\Delta x_{\text{mi}}^t \stackrel{\text{def}}{=} \alpha \cdot g_{\text{mi}}^t. \quad (34)$$

In this way, the perturbation can be written as follows.

$$\delta_{\text{mi}}^t = \Delta x_{\text{mi}}^1 + \Delta x_{\text{mi}}^2 + \cdots + \Delta x_{\text{mi}}^{t-1}. \quad (35)$$

Lemma 4. *The update of the perturbation with the MI attack at step t defined in Equation (34) can be written as $\Delta x_{\text{mi}}^t = \alpha \left[I + \alpha \frac{t-1}{2} H(x) + \mathcal{R}_1^t(H(x)) \right] g(x) + \tilde{R}_1^t$, where $\mathcal{R}_1^t(H(x))$ denotes terms of elements in $H(x)$ higher than the first order, and \tilde{R}_1^t denotes terms with elements in δ_{mi}^{t-1} of higher than the first order.*

Proof. If $t = 1$, $\Delta x_{\text{mi}}^1 = \alpha \cdot g(x)$.

Let $\forall t' < t$, $\Delta x_{\text{mi}}^{t'} = \alpha \left[I + \alpha \frac{t'-1}{2} H(x) + \mathcal{R}_1^{t'}(H(x)) \right] g(x) + \tilde{R}_1^{t'}$.

According to Equation (33) and Equation (34), we have

$$\Delta x_{\text{mi}}^t = \alpha \cdot \left[\frac{t-1}{t} g_{\text{mi}}^{t-1} + \frac{1}{t} g(x + \delta_{\text{mi}}^{t-1}) \right].$$

Applying the Taylor series to the term of $g(x + \delta_{\text{mi}}^{t-1})$, we get

$$\Delta x_{\text{mi}}^t = \alpha \cdot \left[\frac{t-1}{t} g_{\text{mi}}^{t-1} + \frac{1}{t} \left[g(x) + H(x) \delta_{\text{mi}}^{t-1} \right] + r_1^{t-1} \right], \quad (36)$$

where r_1^{t-1} denotes terms of elements in δ_{mi}^{t-1} of higher than the first order.

According to Equation (35) and Equation (36), we get

$$\Delta x_{\text{mi}}^t = \alpha \cdot \left\{ \frac{t-1}{t} g_{\text{mi}}^{t-1} + \frac{1}{t} \left[g(x) + H(x) \left[\Delta x_{\text{mi}}^1 + \Delta x_{\text{mi}}^2 + \cdots + \Delta x_{\text{mi}}^{t-1} \right] \right] + r_1^{t-1} \right\}.$$

Because $\forall t' < t$ $\Delta x_{\text{mi}}^{t'} = \alpha \left[I + \alpha \frac{t'-1}{2} H(x) + \mathcal{R}_1^{t'}(H(x)) \right] g(x) + \tilde{R}_1^{t'}$, we have $\Delta x_{\text{mi}}^{t-1} = \alpha \cdot \left[I + \alpha \frac{t-2}{2} H(x) + \mathcal{R}_1^{t-1}(H(x)) \right] g(x) + \tilde{R}_2^{t-1}$. According to Equation (34), we get $g_{\text{mi}}^{t-1} = \left[I + \alpha \frac{t-2}{2} H(x) + \mathcal{R}_1^{t-1}(H(x)) \right] g(x) + \tilde{R}_2^{t-1}$.

In this way, we get

$$\begin{aligned}
\Delta x_{\text{mi}}^t &= \alpha \cdot \left\{ \frac{t-1}{t} \left[I + \alpha \frac{t-2}{2} H(x) + \mathcal{R}_1^{t-1}(H(x)) \right] g(x) \right. \\
&\quad \left. + \frac{1}{t} \left[I + H(x) \left[\alpha(t-1) + \alpha \frac{(t-2)(t-1)}{4} H(x) + \sum_{t'=1}^{t-1} \mathcal{R}_1^{t'}(H(x)) \right] g(x) + \sum_{t'=1}^{t-1} \tilde{R}_1^{t'} \right] \right. \\
&\quad \left. + r_1^{t-1} \right\} \\
&= \alpha \cdot \left[\underbrace{\frac{t-1}{t} \mathcal{R}_1^{t-1}(H(x)) + \frac{(t-2)(t-1)}{4t} H^2(x) + \frac{1}{t} H(x) \sum_{t'=1}^{t-1} \mathcal{R}_1^{t'}(H(x))}_{\mathcal{R}_1^t(H(x))} \right. \\
&\quad \left. + I + \alpha \frac{t-1}{2} H(x) + \right] g(x) + \underbrace{\frac{1}{t} \sum_{t'=1}^{t-1} \tilde{R}_1^{t'} + r_1^{t-1}}_{\tilde{R}_1^t} \\
&= \alpha \left[I + \alpha \frac{t-1}{2} H(x) + \mathcal{R}_1^t(H(x)) \right] g(x) + \tilde{R}_1^t.
\end{aligned}$$

where $\mathcal{R}_1^t(H(x))$ denotes terms of elements in $H(x)$ higher than the first order, and \tilde{R}_1^t denotes terms with elements in δ_{mi}^{t-1} of higher than the first order. In this way, we have proved that $\forall t \geq 1$, $\Delta x_{\text{mi}}^t = \alpha \left[I + \alpha \frac{t-1}{2} H(x) + \mathcal{R}_1^t(H(x)) \right] g(x) + \tilde{R}_1^t$. \square

Proposition 3. Given an input sample $x \in \mathbb{R}^n$ and a DNN $h(\cdot)$ trained for classification, the adversarial perturbation generated by multi-step attack is denoted by $\delta_{\text{multi}}^m = \alpha \sum_{t=0}^{m-1} \nabla_x \ell(h(x + \delta_{\text{multi}}^t), y)$. The adversarial perturbation generated by multi-step attack incorporating the momentum is computed as $\delta_{\text{mi}}^m = \alpha \sum_{t=0}^{m-1} g_{\text{mi}}^t$. Perturbation units of δ_{mi}^m exhibit smaller interactions than δ_{multi}^m , i.e. $\mathbb{E}_{ij} [I_{ij}(\delta_{\text{mi}}^m)] \leq \mathbb{E}_{ij} [I_{ij}(\delta_{\text{multi}}^m)]$.

Proof. According to Lemma 4, the update of the perturbation with the MI attack at the step t is given as follows.

$$\Delta x_{\text{mi}}^t = \alpha \left[I + \alpha \frac{t-1}{2} H(x) + \mathcal{R}_1^t(H(x)) \right] g(x) + \tilde{R}_1^t. \quad (37)$$

where $\mathcal{R}_1^t(H(x))$ denotes terms of elements in $H(x)$ of higher than the first order. \tilde{R}_1^t denotes terms with elements in δ_{mi}^{t-1} of higher than the first order.

To simplify the notation without causing ambiguity, we write $g(x)$ and $H(x)$ as g and H , respectively. In this way, according to Equation (35) and Equation (37), δ_{mi}^m can be written as follows.

$$\delta_{\text{mi}}^m = \alpha \left[mI + \frac{\alpha m(m-1)}{4} H + \sum_{t=1}^m \mathcal{R}_1^t(H) \right] g + \sum_{t=1}^m \tilde{R}_1^t. \quad (38)$$

where m represents the total number of steps. According to Lemma 1, the Shapley interaction between perturbation units a, b in δ_{mi}^m is given as follows.

$$I_{ab}(\delta_{\text{mi}}^m) = \delta_{\text{mi},a}^m H_{ab} \delta_{\text{mi},b}^m + \tilde{R}_2(\delta_{\text{mi}}^m), \quad (39)$$

where $\tilde{R}_2(\delta_{\text{mi}}^m)$ denotes terms with elements in δ_{mi} of higher than the second order.

According to Equation (38) and Equation (39), we get

$$\begin{aligned} I_{ab}(\delta_{\text{mi}}^m) &= H_{ab} \left[\alpha m g_a + \frac{\alpha^2 m(m-1)}{4} \sum_{b'=1}^n (H_{ab'} g_{b'}) + \cdots + \sum_{t=1}^m \underbrace{o(\delta_{\text{mi},a}^t)}_{\substack{\text{terms of } \delta_{\text{mi},a}^t \\ \text{of higher than the first order,} \\ \text{which corresponds to the term of} \\ \tilde{R}_1^t \text{ in Equation (38)}}} \right] \\ &\quad + \alpha m g_b + \frac{\alpha^2 m(m-1)}{4} \sum_{a'=1}^n (H_{a'b} g_{a'}) + \cdots + \sum_{t=1}^m \underbrace{o(\delta_{\text{mi},b}^t)}_{\substack{\text{terms of } \delta_{\text{mi},b}^t \\ \text{of higher than the first order,} \\ \text{which corresponds to the term of} \\ \tilde{R}_1^t \text{ in Equation (38)}}} \Big] + \tilde{R}_2(\delta_{\text{mi}}^m) \\ &= \underbrace{\alpha^2 m^2 g_a g_b H_{ab}}_{\text{first-order terms w.r.t. elements in } H} \\ &\quad + \underbrace{\left[\frac{\alpha^3(m-1)m^2}{4} g_b \sum_{b'=1}^n (H_{ab'} g_{b'}) + \frac{\alpha^3(m-1)m^2}{4} g_a \sum_{a'=1}^n (H_{a'b} g_{a'}) \right] H_{ab}}_{\text{second-order terms w.r.t. elements in } H} \\ &\quad + \underbrace{\left[\frac{\alpha^4(m-1)^2 m^2}{16} \sum_{b'=1}^n (H_{ab'} g_{b'}) \sum_{a'=1}^n (H_{a'b} g_{a'}) H_{ab} + \cdots \right]}_{\mathcal{R}_2^{\text{mi}}(H)} \\ &\quad + \underbrace{\left[\sum_{t=1}^m o(\delta_{\text{mi},a}^t) H_{ab} \delta_{\text{mi},b}^m + [o(\delta_{\text{mi},b}^t)] H_{ab} \delta_{\text{mi},a}^m + \tilde{R}_2(\delta_{\text{mi}}^m) \right]}_{\tilde{R}_2'(\delta_{\text{mi}}^m)} \\ &= \alpha^2 m^2 g_a g_b H_{ab} + \frac{\alpha^3(m-1)m^2}{4} g_a H_{ab} \sum_{a'=1}^n (H_{a'b} g_{a'}) \\ &\quad + \frac{\alpha^3(m-1)m^2}{4} g_b H_{ab} \sum_{b'=1}^n (H_{ab'} g_{b'}) + \tilde{R}_2'(\delta_{\text{mi}}^m) + \mathcal{R}_2^{\text{mi}}(H), \end{aligned} \quad (40)$$

where $\mathcal{R}_2^{\text{mi}}(H)$ denotes terms of elements in H higher than the second order, and $\tilde{R}_2'(\delta_{\text{mi}}^m)$ denotes terms of elements in δ_{mi}^m higher than the second order

According to Equation (23) and Equation (40), the expectation of the difference between $I_{ab}(\delta_{\text{mi}}^m)$ and $I_{ab}(\delta_{\text{multi}}^m)$ is given as follows.

$$\begin{aligned} &\mathbb{E}_{a,b} [I_{ab}(\delta_{\text{mi}}^m) - I_{ab}(\delta_{\text{multi}}^m)] \\ &= -\frac{\alpha^3(m-1)m^2}{4} \mathbb{E}_{a,b} \left[\underbrace{g_a H_{ab} \sum_{a'=1}^n (H_{a'b} g_{a'})}_{U_{ab}} + \underbrace{g_b H_{ab} \sum_{b'=1}^n (H_{ab'} g_{b'})}_{U_{ba}} \right] + \mathbb{E}_{a,b} [R_{ab}^{\text{mi}}], \end{aligned}$$

where

$$R_{ab}^{\text{mi}} = \tilde{R}_2'(\delta_{\text{mi}}^m) - \tilde{R}_2'(\delta_{\text{multi}}^m) + \mathcal{R}_2^{\text{mi}}(H) - \mathcal{R}_2^{\text{multi}}(H).$$

According to Assumption 1, we have $\mathcal{R}_2^{\text{mi}}(H) \approx 0$, and $\mathcal{R}_2^{\text{multi}}(H) \approx 0$. Note that the magnitude of δ_{mi}^m and the magnitude of δ_{multi}^m are small, then $\tilde{R}_2'(\delta_{\text{mi}}^m) \approx 0$, and $\tilde{R}_2'(\delta_{\text{multi}}^m) \approx 0$. Therefore,

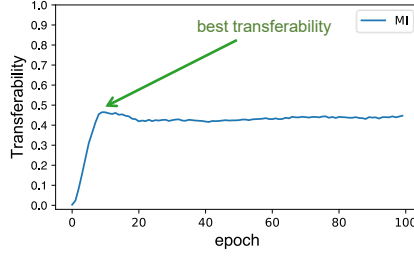


Figure 7: The curve of transferability in different steps.

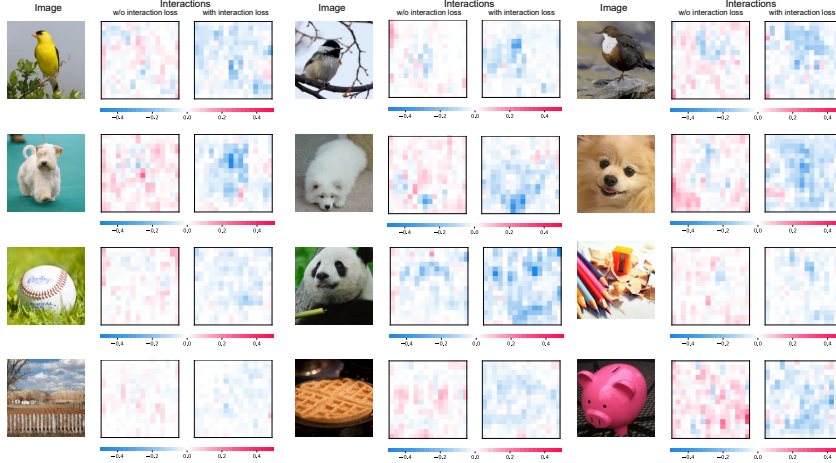


Figure 8: Visualization of interactions between neighboring perturbation units generated with and without the interaction loss. The color in the visualization is computed as $color[i] \propto E_{j \in N_i} [I_{ij}(\delta)]$, where N_i denotes the set of adjacent perturbation units of the perturbation unit i . Here, we ignore interactions between non-adjacent units to simplify the visualization. It is because adjacent units usually encode much more significant interactions than other units. The interaction loss forces the perturbation to encode more negative interactions.

$\mathbb{E}_{a,b} [R_{ab}^{\text{mi}}] = \mathbb{E}_{a,b} [\hat{R}'_2(\delta_{\text{mi}}^m) - \tilde{R}'_2(\delta_{\text{multi}}^m) + \mathcal{R}_2^{\text{mi}}(H) - \mathcal{R}_2^{\text{multi}}(H)] \approx 0$. Moreover, similar to Equation (25) in the proof of Proposition 1, we have $\mathbb{E}_{a,b} [U_{ab}] = \mathbb{E}_{a,b} [U_{ba}] \geq 0$.

Therefore,

$$\begin{aligned}
 & \mathbb{E}_{a,b} [I_{ab}(\delta_{\text{mi}}) - I_{ab}(\delta_{\text{multi}})] \\
 &= -\frac{\alpha^3(m-1)m^2}{4} \mathbb{E}_{a,b} [U_{ab} + U_{ba}] + \mathbb{E}_{a,b} [R_{ab}^{\text{mi}}] \\
 &\approx -\frac{\alpha^3(m-1)m^2}{2} \mathbb{E}_{a,b} [U_{ab}] + 0 \leq 0.
 \end{aligned}$$

□

Note that Proposition 3 just shows the revised MI Attack usually decreases the interaction between perturbation units. The proof towards all types of MI Attacks is still a challenge.

K ADDITIONAL RELATED WORK

Some studies paid attention to intermediate features to improve transferability. Activation Attack (Inkawich et al., 2019) forced the intermediate features of the input image to be similar with the intermediate features of a target image, in order to generate highly transferable targeted example.

Distribution Attack (Inkawhich et al., 2020) explicitly modeled the feature distribution of each class, and improve the targeted transferability by driving the feature of perturbed input image into the distribution of a specific target class. Intermediate Level Attack (Huang et al., 2019) improved the transferability of an adversarial example by maximizing the feature perturbation of a pre-specified layer. In comparison, we explain and improve the transferability based on game theory. Moreover, we discover the negative correlation between the transferability and interactions.

L IMPLEMENTATION OF THE INTERACTION-REDUCED ATTACK (IRA)

As Appendix G mentions, to reduce the computational cost, we can measure interactions between grids, instead of input units (pixels). We divide the entire input image x into $L \times L$ grids, denoted by $\Lambda = \{\Lambda_{11}, \Lambda_{12}, \dots, \Lambda_{LL}\}$. Moreover, we use a sampling method to further reduce the computational cost in a batch manner. In each batch, we approximate the expectation of the interaction as follows.

$$\begin{aligned} & \mathbb{E}_{(p,q),(p',q')} [I_{(p,q),(p',q')}(\delta)] \\ &= \frac{1}{L^2 - 1} \mathbb{E}_{(p,q)} [v(\Lambda) - v(\Lambda \setminus \{\Lambda_{pq}\}) - v(\{\Lambda_{pq}\}) + v(\emptyset)] \\ &= \frac{1}{L^2 - 1} \mathbb{E}_{batch} \mathbb{E}_{(p,q) \in batch} [v(\Lambda) - v(\Lambda \setminus \{\Lambda_{pq}\}) - v(\{\Lambda_{pq}\}) + v(\emptyset)] \\ &\approx \frac{1}{L^2 - 1} \mathbb{E}_{batch} [v(\Lambda) - v(\Lambda \setminus \Lambda_{batch}) - v(\Lambda_{batch}) + v(\emptyset)] \quad \backslash \backslash batchsize \ll L^2 \end{aligned} \quad (41)$$

In this way, Equation (5) can be approximated as

$$\ell(h(x + \delta), y) - \lambda \cdot \frac{1}{K} \sum_{k=1}^K [v(\Lambda) - v(\Lambda \setminus \Lambda_{batch}) - v(\Lambda_{batch}) + v(\emptyset)] \quad (42)$$

where K denotes the sampling times, and $\Lambda_{batch} \subseteq \Lambda$ is a random set with $batchsize$ grids. As a toy example, $\Lambda_{batch} = \{\Lambda_{11}, \Lambda_{35}, \Lambda_{97}\}$ has $batchsize = 3$. In our experiments, we set $L = 16$, $K = 32$, and $batchsize = 32$. Note that we omit the constant $\frac{1}{L^2 - 1}$ in the interaction loss for simplicity.

M EVALUATION OF THE TRANSFERABILITY VIA LEAVE-ONE-OUT VALIDATION

As Fig. 7 shows, the highest transferability of the MI Attack is achieved in an intermediate step, rather than in the last step. This phenomenon presents a challenge for fair comparisons of the transferability between different attacking methods.

To this end, in order to enable fair comparisons of transferability between different methods, we estimate the adversarial perturbations with the highest transferability for each input image via the leave-one-out (LOO) validation as follows. Given a set of clean examples $\{(x_i, y_i)\}_{i=1}^N$, where $y_i \in \{1, 2, \dots, C\}$, we use x_i^t to denote the adversarial example at step t w.r.t. the clean example x_i , where $t \in \{1, 2, \dots, T\}$, and T is the number of total step. Given a target DNN $h(\cdot)$ and an input example x , where $h(\cdot)$ denotes the output before the softmax layer, we use $\mathcal{C}(x) = \arg \max_k h_k(x)$, $k \in \{1, \dots, C\}$ to denote the prediction of the example x .

$$\hat{x}_i \stackrel{\text{def}}{=} x_i^{t_i^*}, \text{ s.t. } t_i^* = \arg \max_t \mathbb{E}_{i' \in \{1, 2, \dots, N\} \setminus \{i\}} [\mathbb{1}[\mathcal{C}(x_{i'}^t) \neq y_{i'}]],$$

where $\mathbb{1}[\cdot]$ is the indicator function. Then the average transferability is given as follows.

$$Transferability = \mathbb{E}_i [\mathbb{1}[\mathcal{C}(\hat{x}_i) \neq y_i]].$$

N ADDITIONAL VISUALIZATIONS OF INTERACTIONS

Figure 2 visualizes interactions between adjacent perturbation units generated with and without the interaction loss. Here, Figure 8 provides more visualization results of interactions between adjacent perturbation units.